A SYNTHESIS OF FLOW PHENOMENA IN HELIUM II

W. DE HAAS

A SYNTHESIS OF FLOW PHENOMENA IN HELIUM II

A SYNTHESIS OF FLOW PHENOMENA IN HELIUM II

PROEFSCHRIFT

TER VERKRIJGING VAN DE GRAAD VAN DOCTOR IN DE WISKUNDE EN NATUURWETENSCHAPPEN AAN DE RIJKSUNIVERSITEIT TE LEIDEN, OP GEZAG VAN DE RECTOR MAGNIFICUS DR. A.E. COHEN, HOOGLERAAR IN DE FACULTEIT DER LETTEREN, VOLGENS BESLUIT VAN HET COLLEGE VAN DEKANEN TE VERDEDIGEN OP WOENSDAG 19 NOVEMBER 1975 TE KLOKKE 14.15 UUR

door

WILLEM DE HAAS
geboren te Leiden in 1942

PROMOTOREN: PROF. DR. K.W. TACONIS
PROF. DR. R. DE BRUYN OUBOTER

DIT PROEFSCHRIFT IS BEWERKT MEDE ONDER TOEZICHT VAN
DR. H. VAN BEELEN

Aan mijn ouders

Aan mijn vrouw

Tekeningen: J. Bij en W.F. Tegelaar
Typografie: E. de Haas-Walraven

Krips Repro - Meppel

TABLE OF CONTENTS

GENERAL INTRODUCTION

The flow properties of He II have been the subject of many investigations over the last four decades, and many experiments on flow through narrow constrictions such as capillaries and slits have been described. The reason for this interest lies in the fact that the properties of He II proved to be quite different from those of a classical liquid, as demonstrated, for instance, by the occurrence of the well-known fountain effect and viscousless flow. It is now well established that a two-fluid model accounts for such observations. This model describes the flow properties of He II on the basis of two interpenetrating but independent flow fields, as though He II consisted of two components, a superfluid and a normal component. The superfluid fraction of the total mass is zero at T_λ = 2.17 K, and increases to one at absolute zero. The superfluid component carries no entropy and its flow field is curlfree; the normal component behaves like an ordinary viscous liquid and carries the entropy.

The most complete set of data on the properties of He II for steady flow can be obtained experimentally by varying the mass flow of the two components independently. All steady flow phenomena observed in different experiments should then in principle be predictable. Such data are obtainable because the mass transport of the normal component corresponds to a heat current that can be imposed independently of the total mass transport.

Strangely enough, only a few experiments have been published in which both the superfluid and the normal components were independently adjusted. So far, most of the experimental information has been gathered from pure heat-conduction experiments, the normal flow being generated by means of a heater, the total mass flow being zero. In some heat-conduction experiments not only the resulting temperature difference is measured but also, simultaneously, the difference in pressure or chemical potential.

Although the experimental data obtained by different authors do not seem to differ greatly, various phenomenological relations have been put forward.

The discrepancies between these relations arise mainly from the specific assumptions made about the contributions of the two components to the observed quantities. To resolve these contributions, one such assumption must always be made, because at least three unknown processes are involved, namely, the interaction of the superfluid and the normal component with the wall as well as their mutual interaction. However, it follows by integration of the well-known relation of Landau:

$$d\mu = \frac{1}{\rho} dP - sdT - \tfrac{1}{2} \frac{\rho_n}{\rho} d(\vec{v}_n - \vec{v}_s)^2$$

that only two of the three measurable differences provide independent information. Therefore, experiments of this kind, in which the macroscopic differences are measured as a function of the transport velocities involved, are too coarse to permit a unique description of the flow. Nevertheless, apart from their direct applicability for the design of apparatus, the experimental results are very useful for the testing of existing hydrodynamic models. Only one experiment has been published as yet - by Van der Heijden et al. - in which two of the three quantities $\Delta\mu$, ΔT, and ΔP were measured systematically as a function of the two independent transport velocities v_n and v_s. The aim of the present research was to carry out such a systematic investigation.

In Chapter I we present our data on the steady adiabatic superfluid transport of He II driven by a set of plungers through capillaries enclosed by two superleaks. In Chapter II we describe how these measurements were extended by allowing the normal transport to be adjusted independently. The general result of $\Delta\mu(v_s,v_n)$ is then used to explain the occurrence of a velocity region in which oscillations in the flow are observed.

Another test of the applicability of the general form of $\Delta\mu(v_s,v_n)$ as well as of $\Delta T(v_s,v_n)$ is given in Chapter III, where a description is given of a flow experiment in a closed circuit in which the condition $\Delta\mu = 0$ is necessarily realized during steady flow. The flow is generated by a heater only. The observed temperature differences are compared with those of the plunger-driven flow (Chapter II) for those velocity combinations where $\Delta\mu = 0$.

Finally, in Chapter IV some considerations on the hydrodynamics of the flow are given and an attempt is made to interpret the experimental results in terms of the dynamic processes taking place in the flow path.

CHAPTER I

SUPERFLUID TRANSPORT ONLY

Synopsis

Measurements are reported on adiabatic superfluid transport through capillaries of different dimensions. The energy dissipation, the chemical potential difference, and the temperature difference over the capillary were measured as a function of the steady-state mass velocity generated by a motor-driven plunger system. The results can be described by the Gorter-Mellink mutual interaction force and an additional superfluid frictional force; no critical velocity was found.

1. Introduction

When He II is forced to flow through a system consisting of two superleaks connected in series by a chamber dissipation in the chamber can take place. This dissipation was measured by Van Alphen et al.[1] calorimetrically, for a number of chamber geometries (capillaries and slits of various widths). From his measurements Van Alphen deduced a.o.:

a) below a critical flow velocity v_{sc} no dissipation in the chamber takes place, where $v_{sc} \approx d^{-\frac{1}{4}}$ with d being the characteristic width of the chamber in cm;

b) above the critical velocity the dissipation varies as the third power of the superfluid velocity, the proportionality constant being dependent on temperature and on the geometry of the flow system.

In order to verify the above statements and to investigate the geometry dependence in more detail we carried out similar experiments in a capillary, using a slightly different technique. Van Alphen deduced the amount of dissipation from the initial rate at which the temperature of the calorimeter increased. We took our data only in the steady state (when also the temperature

in the chamber had reached its final value), in order to be sure that the influence of transient effects is avoided. Moreover, at each flow velocity we did not only measure the dissipation rate $\dot{E}$ but also the temperature difference ΔT and the chemical-potential difference $\Delta\mu$ over the capillary; $\Delta\mu$ equals $-g\Delta Z$ owing to the well-established fact that the chemical-potential difference over a superleak is zero. Measuring runs at different bath temperatures were carried out using stainless-steel and copper capillaries of various lengths and diameters.

2. The experimental set-up

Fig. 1 shows a schematic diagram of the apparatus, the capillary C and

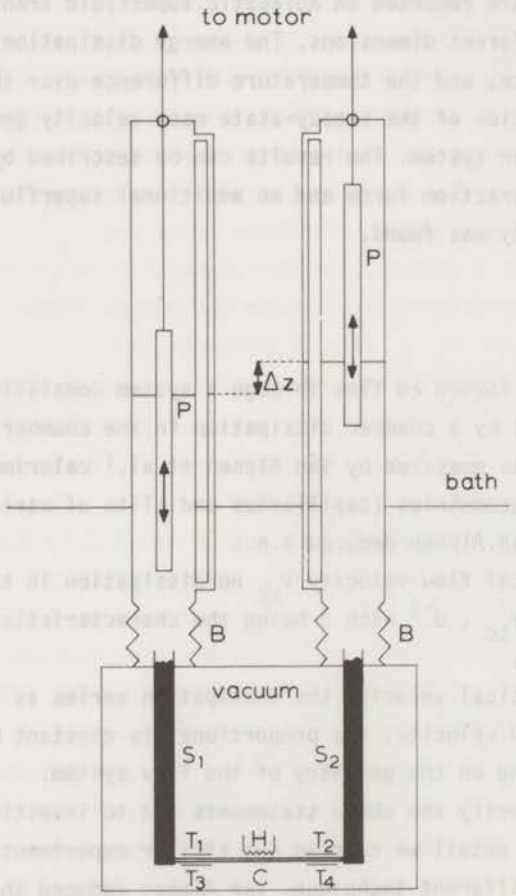

Fig. 1 *Schematic drawing of the apparatus. C: capillary; S: superleak; B: bellows; H: heater; T: carbon thermometer; P: plunger.*

the superleaks S_1 and S_2 being enclosed by a vacuum can. The flow is generated by a motor-driven plunger system. We have chosen for a symmetric construction in order to avoid a zero flow due to the evaporation of the bath. The bellows B at both superleaks provide good thermal contact with the bath, so that there will not be a temperature difference over the flow system. Using identical superleaks S_1 and S_2 with the same heat resistance, the energy-dissipation rate $\dot{E}$ in the capillary is measured by the two identical carbon thermometers T_1 and T_2. The change in their total resistance $\Delta(R_1 + R_2)$ is calibrated as a function of the heat input by means of a heater H. ΔZ is read by a cathetometer. The temperature difference over the capillary, $\Delta T = T_4 - T_3$ is measured differentially in a Wheatstone bridge.

The measurements were carried out using the following capillaries:

a) three stainless-steel capillaries all with an inner diameter of 0.10 cm, outer diameter 0.15 cm and with a length of 4.5, 10, and 20 cm, respectively;

b) a stainless-steel capillary with an inner diameter of 0.034 cm, outer diameter 0.060 cm and with a length of 10 cm;

c) a copper capillary with an inner diameter of 0.10 cm, outer diameter 0.20 cm and with a length of 10 cm.

3. Experimental results

A typical example of the measured dissipation rate $\dot{E}$ as a function of the superfluid velocity v_s in the capillary is given in Fig. 2. For all measuring runs these graphs look very similar to those found by Van Alphen, the dissipation being of the same order of magnitude. It follows from thermodynamics that[2]

$$\dot{E} = -\rho O v \Delta\mu = \rho O v g \Delta Z \quad , \tag{1}$$

in which O is the cross-sectional area of the capillary. Figs. 3a and b show that this energy relation is well obeyed proving that our measurements of $\dot{E}$ and ΔZ are consistent. Figs. 4a up to 4f show the linear dependence of $g\Delta Z$ on v^3 implying $\dot{E} \sim v^4$, contrary to $\dot{E} \sim v^3$ measured by Van Alphen and others[1,12,14]. Furthermore the value $v_{sc} = d^{-\frac{1}{4}}$ is indicated showing that at least in our narrow-capillary experiment no trace of such a critical velocity is found. (Owing to the small value of $d^{-\frac{1}{4}}$ the experimental evidence for the absence of v_{sc} in the wide capillary is less conclusive.) The above conclusions

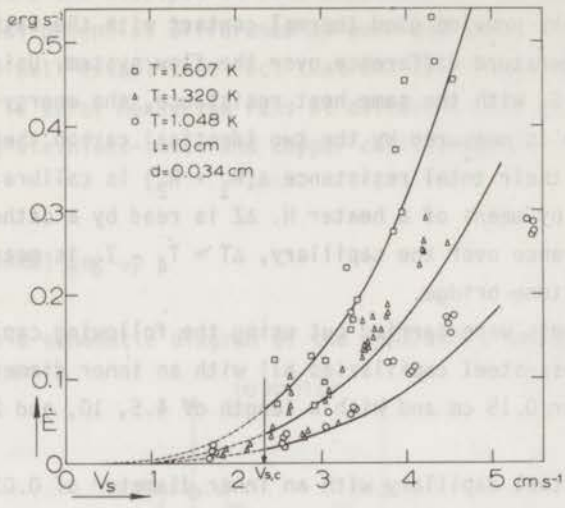

Fig. 2 *Dissipation rate $\dot{E}$ against superfluid velocity v_s. The solid lines represent the relation $\dot{E} = \frac{1}{2}B\Omega l v_s^3$, the value of B taken from the measurements of Van Alphen et al.*[1] *The critical velocity $v_{sc} = d^{-\frac{1}{2}}$ is also indicated.*

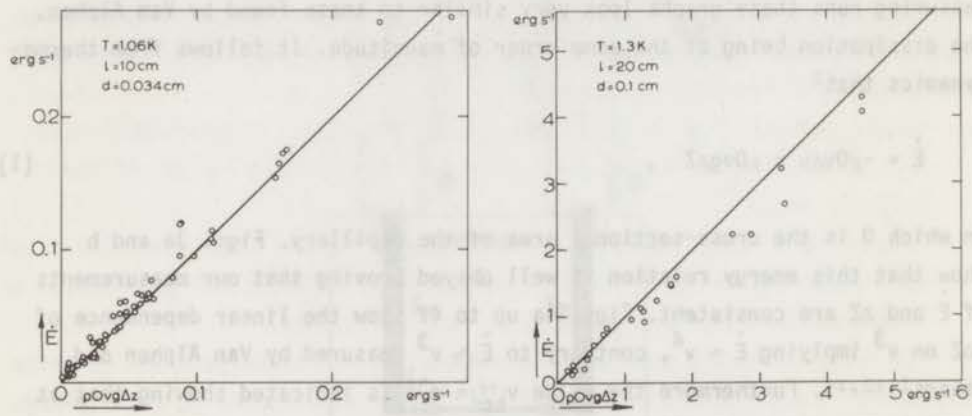

Fig. 3a,b *Dissipation rate $\dot{E}$ against $\rho\Omega vg\Delta Z$ for two of the steel capillaries.*

apply to all our measuring runs.

The measured temperature difference over the capillary is also shown in Figs. 4, the highest temperature occurring at the downstream side of the capillary. For the higher bath temperatures the data of $s\Delta T$ almost coincide with those of $g\Delta Z$ implying that ΔP over the capillary is small compared to the absolute value of $g\Delta Z$ and $s\Delta T$ (see Figs. 4e and 4f).

We should like to remark here that in view of this result one could wonder what would happen if the flow conditions in the capillary were isothermal, would a critical velocity occur in that case? In order to find the answer to this question experimentally we used our thin-walled stainless-steel capillary, while contact gas was let into the vacuum chamber. Though, naturally, ΔT on the outside wall of the capillary now remained zero, no change in the data of $g\Delta Z$ as a function of v was found. This result can be understood from the presence of the well-known Kapitza resistance[3,13,15] between the He in the capillary and the capillary wall. A small circulation of heat, transported by the He in the capillary with $v_n < 0.01$ v, and flowing back through the exchange gas, is sufficient to maintain the temperature difference in the helium while the capillary wall is at a uniform temperature. It therefore appears impossible to carry out this type of experiment isothermally.

Figs. 4 show that at lower bath temperatures $s\Delta T$ becomes smaller than $g\Delta Z$. It does not seem possible to explain the relative decrease of ΔT (as compared to ΔZ) along the same lines as sketched for the "quasi-isothermal" case with heat now flowing back through the capillary wall only. In spite of the much higher Kapitza resistance at these lower bath temperatures so that only a small circulation of heat is needed to explain the decrease of ΔT on the outside wall, a simple calculation shows that the heat conductivity of the stainless-steel wall is still too poor[15]. One therefore has to conclude that a pressure drop over the capillary

$$\Delta P_{cap} = -\rho g \Delta Z + \rho s \Delta T \qquad (2)$$

does occur.

The results for the copper capillary are very similar although in this case $s\Delta T < g\Delta Z$ even at a bath temperature of 1.6 K. This difference can be well explained by the circulation of heat over the Kapitza resistance back through the capillary wall, owing to the good heat conductivity of copper. A velocity of the normal component in the capillary $v_n < 0.01$ v is again sufficient.

As for the proportionality factors α and β, defined by $g\Delta Z \equiv \alpha v^3$ and

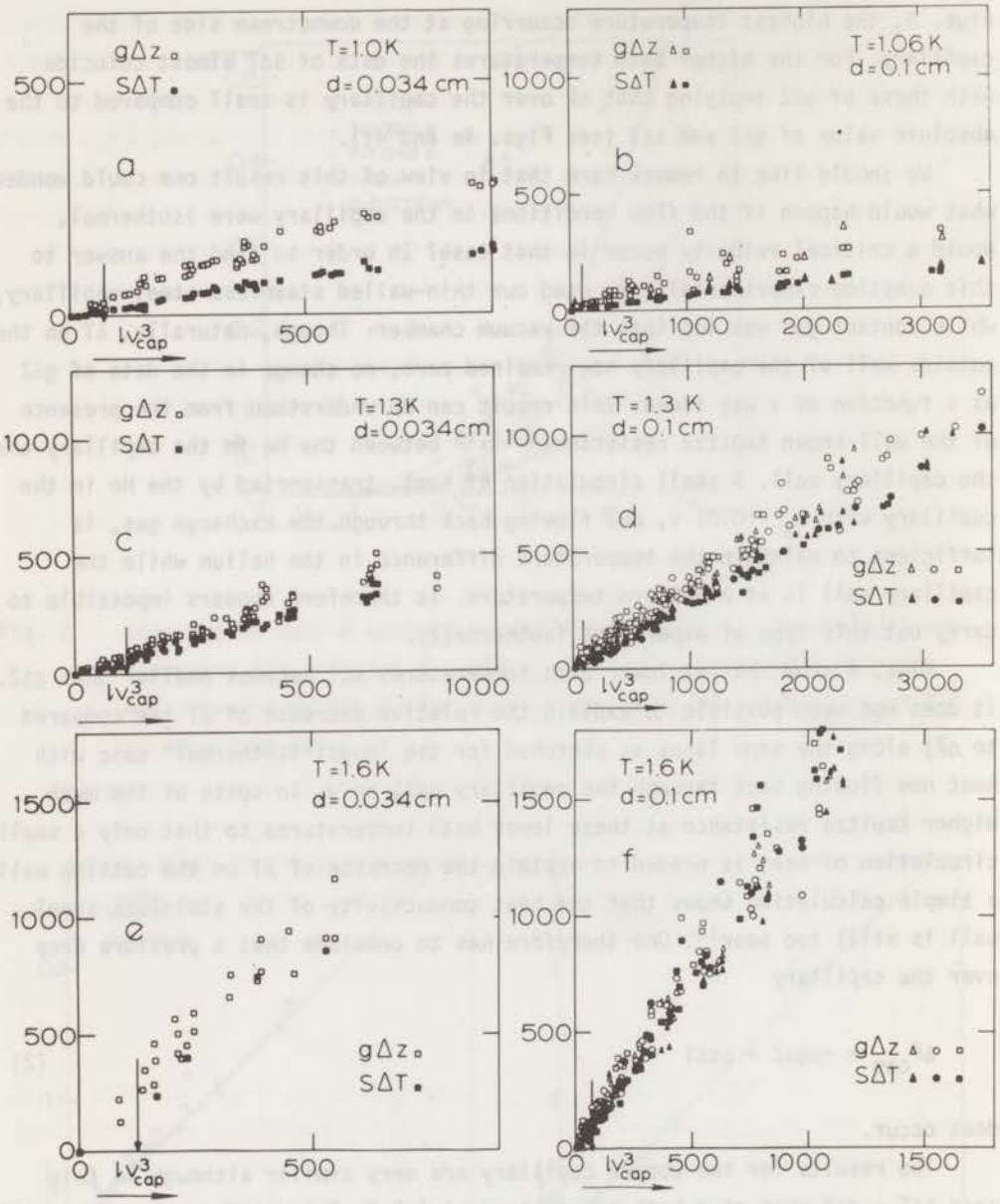

Fig. 4 *gΔZ and sΔT (in $cm^2 s^{-2}$) against lv_{cap}^3 (in $cm^4 s^{-3}$) for all steel capillaries. For the 0.034 cm i.d. capillary the length $l = 10$ cm. For the 0.1 cm i.d. capillaries $l = 4.5$ cm (squares), $l = 10$ cm (circles), and $l = 20$ cm (triangles). The arrows indicate the value $v_{sc} = d^{-\frac{1}{4}}$.*

$s\Delta T \equiv \beta v^3$, α and β appear to be nicely proportional to the length of the capillary at a given bath temperature, as follows from all results of the 0.10 cm i.d. stainless-steel capillaries of 4.5, 10, and 20 cm length (see Figs. 4b, 4d, and 4f where we have plotted $g\Delta Z$ and $s\Delta T$ against lv^3); this indicates that end-effects can be neglected. From a comparison of the results in the 0.10 cm and 0.03 cm i.d. stainless-steel capillaries it can be concluded that α and β increase with decreasing diameter. The value of α and β for the copper and steel capillary turn out to be equal (see also Fig. 5). A discussion of the temperature dependence of α and β will be given in the next paragraph.

4. Discussion of the results

The proportionality of the chemical-potential difference $g\Delta Z$ with the cube of the mass-flow velocity v suggests a description in terms of a mutual interaction of the Gorter-Mellink type[4]

$$F_{sn} = A\rho_s\rho_n(v_s - v_n)^3 \quad , \tag{3}$$

where F_{sn} is the mutual interaction force per unit volume, averaged over the cross-section of the capillary, and v_s and v_n are the mean transport velocities of the superfluid and normal component. A is a proportionality constant which is usually found[5] to be of the order of 50 cm s g^{-1}.

The equations of motion for the local normal and superfluid component in the limit of small velocities are often written as[6,7]

$$\rho_s \frac{\partial \vec{v}_s}{\partial t} + \rho_s \vec{v}_s \cdot \vec{\nabla}\vec{v}_s = -\rho_s \vec{\nabla}\mu \tag{4}$$

and

$$\rho_n \frac{\partial \vec{v}_n}{\partial t} + \rho_n \vec{v}_n \cdot \vec{\nabla}\vec{v}_n = -\frac{\rho_n}{\rho}\vec{\nabla}P - \rho_s s\vec{\nabla}T + \eta\nabla^2\vec{v}_n \quad . \tag{5}$$

For the measured transport velocities v_s and v_n, which are an average over time and cross-section of the local velocities $\vec{v}_s$ and $\vec{v}_n$, these equations are often written as[8,9]

$$\rho_s \frac{\partial v_s}{\partial t} = -\rho_s \frac{d\mu}{dx} - F_{sn} - F_s \quad , \tag{6}$$

$$\rho_n \frac{\partial v_n}{\partial t} = -\frac{\rho_n}{\rho}\frac{dP}{dx} - \rho_s s \frac{dT}{dx} + F_{sn} - F_n \quad . \tag{7}$$

For steady-state conditions and $v_n \approx 0$ integration along the transport direction yields

$$0 = -\rho_s \Delta\mu - F_{sn} l - F_s l \quad , \tag{8}$$

$$0 = -\frac{\rho_n}{\rho} \Delta P - \rho_s s \Delta T + F_{sn} l \quad , \tag{9}$$

where we have neglected all terms of order $\Delta T/T$ by taking for the temperature-dependent quantities ρ_s, ρ_n, s, F_{sn}, and F_s their value at the temperature T_{bath}.

Equations (8) and (9) can be rewritten as

$$F_{sn} l = -\rho_n g \Delta Z + \rho s \Delta T = (-\rho_n \alpha + \rho\beta) v^3 \approx \rho_s \beta v^3 \quad , \tag{10}$$

$$F_s l = \rho g \Delta Z - \rho s \Delta T = \rho(\alpha - \beta) v^3 \quad . \tag{11}$$

A can directly be obtained from plots of $s\Delta T$ against v^3 as $\rho_n(\alpha - \beta)$ can be neglected for all temperatures (see Figs. 4a up to f). Fig. 5 shows A calculated

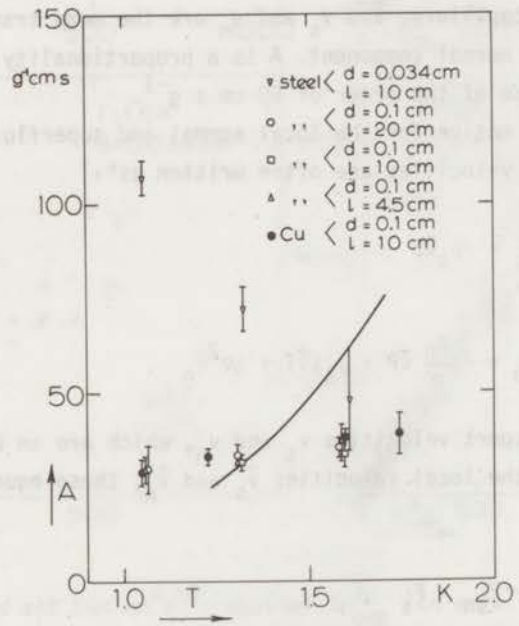

Fig. 5 *Gorter-Mellink proportionality constant A against temperature. The solid line represents the measurements of Vinen*[16].

from eqs. (3) and (10) as a function of temperature for the different capillaries. From this Figure it follows that for the 0.1 cm i.d. capillary A is only weakly dependent on temperature, proving that the temperature dependence of F_{sn} is mainly accounted for by the factor $\rho_n\rho_s(\rho/\rho_s)^3$. The coincidence of A for the three stainless-steel capillaries of different length demonstrates the proportionality with l. We like to draw attention to the value of A being the same for the 0.1 cm i.d. stainless-steel and copper capillaries, if properly corrected for heat conduction and Kapitza resistance. The different temperature dependence for the 0.03 cm i.d. stainless-steel capillary is not understood[10].

From the linear character of both curves in Figs. 4 the same length and velocity dependence for F_s as for F_{sn} follows[11]. At T is 1.6 K it appears that $F_s/F_{sn} \ll 1$, while at T = 1.0 K this ratio has increased to order unity, mainly due to the decrease of F_{sn}.

The above discussion leads to the conclusion that a phenomenological description of the flow properties of He II in terms of a Gorter-Mellink mutual interaction is in qualitative agreement with the measurements, if one allows for an additional friction force on the superfluid transport only. The introduction of this additional friction force in order to interpret the experimental data is a necessary consequence of the implicitly made assumption that the friction of the normal component is zero when the transport of the normal component is zero. As is stated in the General Introduction such an assumption about the forces F_{sn}, F_s, and F_n has to be made in order to resolve them from the experimental data.

In the next Chapter where measurements are presented for flow at independently adjustable transport velocities for the superfluid and normal component, we will make use of the impossibility to distinguish experimentally between F_s and F_n and change our point of view by choosing for the assumption that the superfluid friction force is always zero, implying that the friction of the normal component can be unequal to zero even when the normal transport velocity is zero.

References

1. Van Alphen, W.M., Thesis, Leiden (1969).
De Bruyn Ouboter, R., Taconis, K.W. and Van Alphen, W.M., Progr. low Temp. Phys., C.J. Gorter, ed. North-Holland Publ. Comp. (Amsterdam, 1967) Vol. 5, Ch. 2.

Van Alphen, W.M., De Bruyn Ouboter, R., Taconis, K.W. and De Haas, W., Physica 40 (1969) 469 (Commun., Leiden, No. 367a).
2. Olijhoek, J.F., Thesis, Leiden (1973) Ch. III (p. 72).
Olijhoek, J.F., Van Beelen, H., De Bruyn Ouboter, R. and Taconis, K.W., Physica 72 (1974) 381 (Commun., Leiden, No. 406b).
3. Wilks, J., The Properties of Liquid and Solid Helium, Clarendon Press (Oxford, 1967) Ch. 14, §9.
4. Gorter, C.J. and Mellink, J.H., Physica 15 (1949) 285 (Commun., Leiden, Suppl. No. 98a).
5. London, F., Superfluids, Vol. II, John Wiley (New York, 1954) Ch. E., §24.
6. Landau, L.D. and Lifshitz, E.M., Fluid Mechanics, Addison Wesley (Reading, Mass., 1959) Ch. XVI.
7. Wilks, J., The Properties of Liquid and Solid Helium, Clarendon Press (Oxford, 1967) Ch. 3, §5.
8. Tough, J.T. and Oberly, C.E., J. low Temp. Phys. 6 (1972) 161.
9. Wilks, J., The Properties of Liquid and Solid Helium, Clarendon Press (Oxford, 1967) Ch. 13, §6.
10. Kramers, H.C., Physica 26 (1960) S81.
11. Van der Heijden, G., Thesis, Leiden (1972) Ch. II.
Van der Heijden, G., Giezen, J.J. and Kramers, H.C., Physica 61 (1972) 566 (Commun., Leiden, No. 394c).
12. Brewer, D.F. and Edwards, D.O., Phil. Mag. 7 (1962) 721.
13. Mittag, K., Cryogenics 13 (1973) 94.
14. Talmi, A. and Landau, J., J. low Temp. Phys. 12 (1973) 275.
15. Chelton, D.B. and Mann, D.B., Cryogenic Data Book, U.S. A.E.C. (1956) p. 86.
16. Vinen, W.F., Proc. Roy. Soc. A240 (1957) 114.

CHAPTER II

COMBINED SUPERFLUID AND NORMAL FLUID TRANSPORT

Synopsis

The measurements on steady adiabatic superfluid flow were extended by allowing the normal transport velocity to be adjusted independently. The chemical-potential difference and the temperature difference over a capillary were measured at two bath temperatures both as a function of the steady mass-flow velocity generated by a motor-driven plunger system and as a function of the normal transport velocity generated by a heater.

The general results for $\Delta\mu$ and ΔT appear to be complicated but smooth functions of (v_s, v_n). For small mass-flow velocities and relatively large normal transport velocities metastable flow states were observed. The general character of $\Delta\mu(v_s, v_n)$ accounts for the occurrence of a velocity region showing instabilities in the flow. The resulting oscillations are discussed in some detail.

1. Introduction

In this Chapter the experimental results for the general steady flow behaviour are presented. Both transport velocities were varied independently. This was achieved by removing one of the superleaks from the apparatus described in Chapter I and by mounting a heater for the generation of the normal flow between the remaining superleak and the capillary. As is stated in the General Introduction, such an experiment renders a systematic set of data for $\Delta\mu(v_s, v_n)$ and $\Delta T(v_s, v_n)$ from which all steady flow phenomena observed in different experiments should originate. For instance, pure heat-conduction experiments ($v = 0$) are included, and also the measurements on superfluid transport only ($v_n = 0$) described in Chapter I.

As far as the quantitative agreement between the results of different

experiments is concerned, the length and diameter dependence of the observed quantities should also be investigated. However, in Chapter I it is found that at least for superfluid transport the observed differences in chemical potential and temperature are proportional to the length of the capillary. From a comparison of the heat-conduction experiments which are reported in the literature it follows that the diameter dependence mainly shows up in Poiseuille's law, but that the general character of the results is not affected by a variation in diameter, at least in the region of a few hundred microns.

We therefore did not undertake the lengthy task to collect also a systematic set of data on the length, diameter, and temperature dependence of the observed quantities but rather focussed our attention on the velocity dependence.

2. Experimental set-up

Figure 1 shows a schematic diagram of the apparatus. It consists of a vacuum can enclosing the superleak S and the glass capillary C. The superleak is a thin-walled stainless-steel tube filled with compressed jewellers rouge. A glass capillary was chosen in order to minimize a possible influence of the roughness of the wall and of end-effects. The carbon thermometers T_1 and T_2 and the heater H were mounted on small copper plugs which were in direct contact with the helium through the glass wall (see inset Figure 1). All metal and glass parts were connected to each other by platinum joints.

Inside the brass cylinders (2 cm i.d.) mounted on the vacuum can two identical plungers can move up and down, driven from outside the cryostat by means of a motor. These plungers are coupled in such a way that if one is raised the other is automatically lowered at the same speed. By using two sets of plungers (0.7 and 1.2 cm diameter and 30 cm length) stationary flow with velocities ranging from 1 to 10 cm s^{-1} could be produced in the investigated capillary of i.d. 216 μm.

The copper bellows B provide good thermal contact with the bath. Glass standpipes are placed along the cylinders to read the level difference ΔZ by a cathetometer. Film flow between the flow system and the surrounding bath is not only symmetric but also effectively eliminated by closing the tops of the brass cylinders except for a 1 mm diameter hole (see Figure 1).

The capillary was carefully selected out of a number of specimens; its variation in the radius is less than 1% as was verified by measuring the length of a mercury column at different places inside it. The radius itself was determined both by a flow experiment of helium gas at room temperature and by

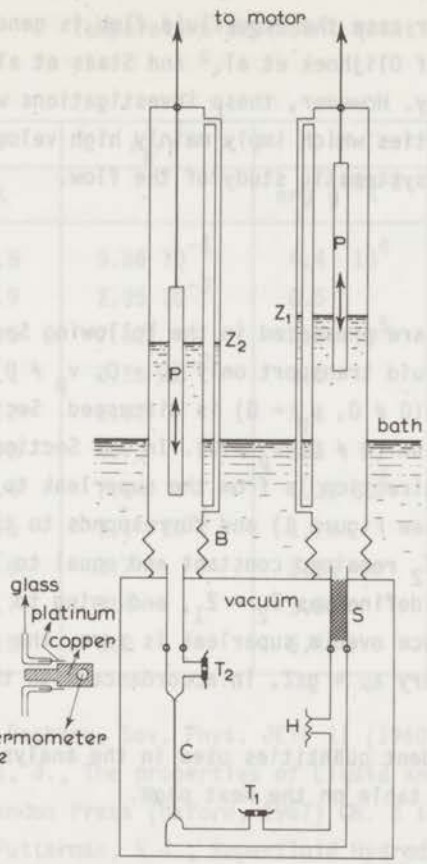

Fig. 1 *Schematic drawing of the apparatus. C: capillary; S: superleak; B: bellows; H: heater; T: carbon thermometer; P: plunger. The inset shows the thermometer- and heater mounting.*

weighing the capillary when filled with mercury. The uncertainty amounts to 1%.

During the measurements the bath temperature was kept constant within a few tenths of a mK using a separate carbon thermometer and a heater. The temperature itself is known within a few mK by a calibration of the thermometers against the vapour pressure of ^{3}He. After adjusting the plunger speed v_p and the heat input $\dot{Q}$ to the desired values the resulting level and temperature differences were determined after the stationary state was reached. The equilibrium state with $v_p = 0$ and $\dot{Q} = 0$ was checked regularly during each measuring day. In this way measurements were carried out at two bath temperatures T = 1.326 and 1.054 K.

Similar experiments were carried out by Van der Heijden et al.[1], the main difference being that in our case the superfluid flow is generated by a set of plungers. The experiments of Olijhoek et al.[2] and Staas et al.[3] were also carried out in a similar way. However, these investigations were aimed at a study of the cooling properties which imply mainly high velocities, and they do not provide primarily a systematic study of the flow.

3. Experimental results

The experimental data are presented in the following Sections: in Section 3.1 the results for superfluid transport only ($\dot{Q} = 0$, $v_p \neq 0$) are given. In Section 3.2 pure heat flow ($\dot{Q} \neq 0$, $v_p = 0$) is discussed. Section 3.3 gives the results for the combined flow ($\dot{Q} \neq 0$, $v_p \neq 0$). In all Sections v_n and v_s are defined positive if their direction is from the superleak to the capillary; ΔT is defined as $T_2 - T_1$ (see Figure 1) and corresponds to the change in T_1 only, as it appeared that T_2 remained constant and equal to T_{bath} at all stages of the measurements. ΔZ is defined as $Z_2 - Z_1$, and owing to the fact that the chemical-potential difference over a superleak is zero, the chemical-potential difference over the capillary $\Delta\mu = g\Delta Z$, in accordance with the definition of the sign of v_{cap} and ΔT.

The temperature-dependent quantities used in the analysis were deduced from the data given in the table on the next page.

3.1 Superfluid transport only

The results of $\rho s\Delta T$ and $\rho\Delta\mu$ produced by the mass flow when no heat is applied are shown in Figures 2a and b. The velocity in the capillary, v_{cap}, was calculated directly from the plunger speed as in a stationary situation the level difference ΔZ is constant in time. The absolute values of $\rho s\Delta T$ and $\rho\Delta\mu$ are plotted against the absolute values of v_{cap}^3 for both flow directions in the same graph, showing the symmetry observed for this type of flow. The actual signs of these quantities during the experiment are such that cooling at T_1 occurs when $v_{cap} > 0$, as is also the case in the work of Olijhoek et al.[2] and in the "vortex cooler" studied by Staas et al.[3]

The present data can also be compared with the results of Chapter I, the only difference being that now the second superleak connecting the capillary with the bath is removed. This should not affect the flow, although the normal component is free to move. The reason is that its transport velocity remains

Temperature-dependent quantities

T	ρ_n/ρ	s	η
K		erg $g^{-1}K^{-1}$	poise
0.8	$9.66\ 10^{-4}$	$4.4\ \ 10^{4}$	$1.58\ 10^{-4}$
0.9	$2.95\ 10^{-3}$	8.5	$6.5\ \ 10^{-5}$
1.0	7.52	$1.64\ 10^{5}$	3.7
1.1	$1.56\ 10^{-2}$	3.0	2.3
1.2	2.92	5.1	1.77
1.3	4.78	8.5	1.6
1.4	7.54	$1.32\ 10^{6}$	1.51
1.5	$1.1\ \ 10^{-1}$	1.96	1.41
1.6	1.7	2.84	1.3
1.7	2.4	3.98	1.28
1.8	3.2	5.45	1.28

ρ_n/ρ : V.P. Peshkov, Sov. Phys. JETP 11 (1960) 580.
Wilks, J., The properties of Liquid and Solid Helium, Clarendon Press (Oxford, 1967) Ch. 3 §4.

S : See Putterman, S.J., Superfluid Hydrodynamics, North-Holland Publ. Co. (Amsterdam, 1974) page 419.

η : A.D.B. Woods and A.C. Hollis-Hallet, Can. J. Phys. 41 (1963) 596.
W.J. Heikkila and A.C. Hollis-Hallet, Can. J. Phys. 33 (1955) 420.

very small (< 0.02 cm s^{-1}) as it is only generated by the energy dissipation $\dot{E}$, so that

$$v_n \leq \frac{\dot{E}}{\rho s T \pi r^2} = - \frac{v \Delta\mu}{sT} \quad .$$

As is shown in Figures 2 the results can indeed be described again by a cubic dependence of $\rho s \Delta T$ and $-\rho\Delta\mu$ on the transport velocity. The pressure differences $\Delta P = \rho\Delta\mu + \rho s \Delta T$ for the two bath temperatures are similar to those found in Chapter I: again at T = 1.326 K ΔP almost disappears compared to the value of $\rho\Delta\mu$, while at T = 1.054 K it amounts to nearly 50%. This is also in

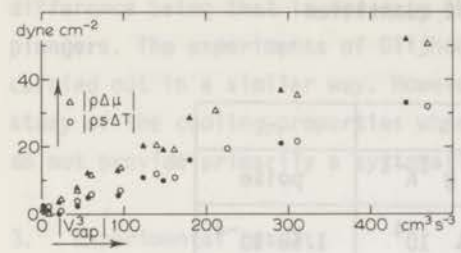

Fig. 2a

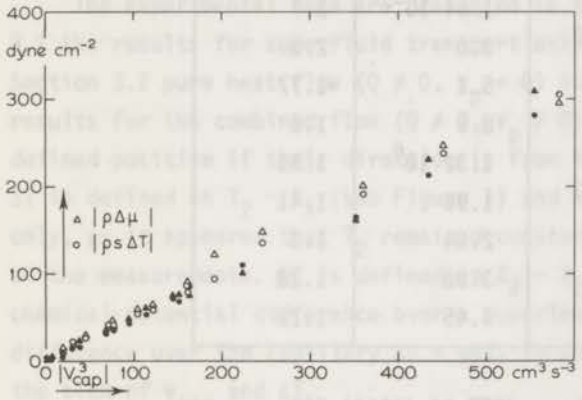

Fig. 2b

Fig. 2a,b *The absolute value of* ρΔμ *and* ρsΔT *against the absolute value of the mass-flow velocity; open symbols correspond with positive, full symbols with negative flow direction. Fig. 2a at T = 1.054 K, Fig. 2b at T = 1.326 K.*

agreement with the findings of Olijhoek et al.[4] who observed that at high temperatures ΔP remained nearly zero.

The proportionality factors of ρsΔT and -ρΔμ with v^3_{cap} are also in quantitative agreement with those reported earlier for the 1000 micron steel and copper capillaries, the corresponding values for the present 216 micron glass capillary being about 25% higher.

3.2 Pure heat conduction (counterflow only)

More than any other type of flow pure heat flow has been the subject of many investigations. In most cases, only the temperature difference as a function of the heat input was measured; only a few experiments are known in which also the corresponding difference in pressure or chemical potential was recorded[5,6,7,8].

With the present apparatus pure heat flow can also be studied as counter-flow will be established once the steady state is reached. Both ΔT and ΔZ were measured up to a maximum heat input which is rather small, due to the long response time of the system at high heat inputs.

Figures 3a and b give the temperature difference over the capillary as a function of the heat input $\dot{Q}$ at the two bath temperatures. As heat is transported only by the normal component, $\dot{Q} = \rho s T \pi r^2 v_n$, we plotted $-\rho s \Delta T$ against v_n. For the temperature-dependent quantities we simply took their value at $T = \frac{1}{2}(T_1 + T_2) = T_{bath} + \frac{1}{2}\Delta T$. In this way the temperature variation along the capillary has been taken into account, as the maximum error which occurs for the largest value of $\Delta T \simeq 10$ mK and at the lowest bath temperature $T_{bath} = 1.054$ K, is still less than 0.05%.

In calculating v_n we corrected for the small heat loss over the superleak and electrical leads. We determined this heat loss in a separate experiment, the capillary being removed. The results were that for

$T_{bath} = 1.326$ K $\qquad \Delta T/\dot{Q} = 7.4 \times 10^{-4}$ K s erg^{-1}

and

$T_{bath} = 1.054$ K $\qquad \Delta T/\dot{Q} = 4.5 \times 10^{-3}$ K s erg^{-1} .

The corrections on v_n due to this heat loss amounted to less than 1½%.

Figures 4a and b give the corresponding chemical-potential difference over the capillary as function of v_n. To show clearly how $\rho\Delta\mu$ approaches zero some data with $\rho\Delta\mu = 0$ have been omitted in this region.

The plots presented in the Figures 3 and 4 show the familiar behaviour as is found by others. Above a certain value of v_n the flow shows a hysteretic behaviour and two branches can be distinguished. The first shows a continuation of the linear relation for $-\rho s \Delta T$ versus v_n and $\rho\Delta\mu = 0$. The other corresponds to a steeper increase of $-\rho s \Delta T$ while simultaneously $\rho\Delta\mu$ increases sharply. The latter branch led Gorter and Mellink to the introduction of the mutual friction force[5]. In the hysteretic region the state corresponding to the linear branch of $-\rho s \Delta T$ becomes clearly metastable. By gently increasing the heat input $\dot{Q}$ it can be traced up to an unpredictable value (which can be as high as 75 cm s^{-1} as was found for $T_b = 1.054$ K) at which $-\Delta T$ and ΔZ suddenly start to rise to their value on the stable higher branch. By subsequently reducing $\dot{Q}$ this second branch is then followed downwards.

In Figures 3b and 4b some additional measuring points are given connected by a line. We found that starting from the second branch another metastable flow state could be observed upon carefully increasing $\dot{Q}$ again.

Results for pure heat conduction; for the points connected by a line in Figs. b, see text.

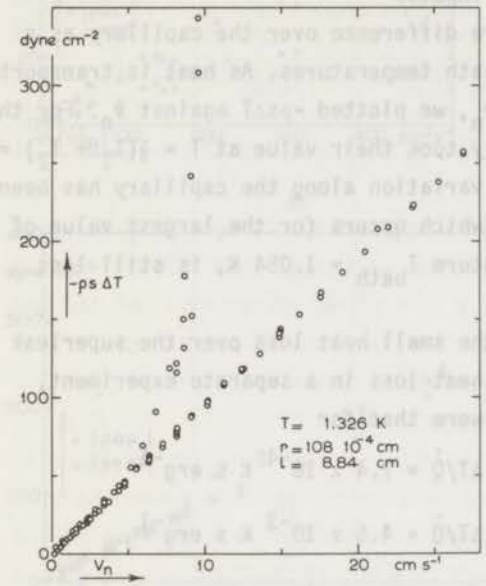

Fig. 3a

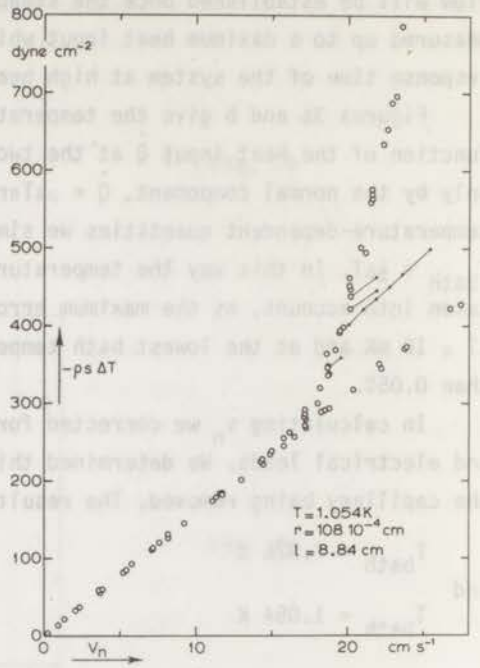

Fig. 3b

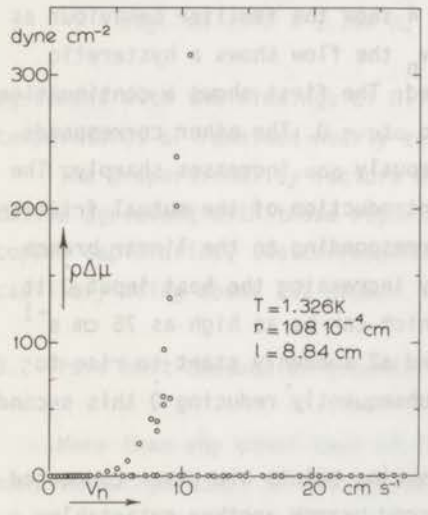

Fig. 4a

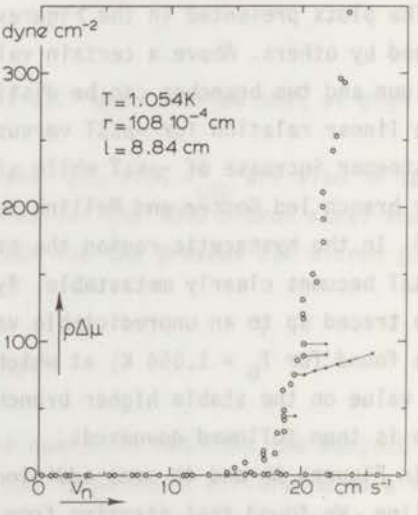

Fig. 4b

Although an analysis of the results in terms of the equations of motion will be postponed to the general discussion of all the results in Section 4 some preliminary remarks will be made here.

The flow regime with $\rho\Delta\mu = 0$ and $-\rho s\Delta T$ proportional to v_n is usually described by a Poiseuille law as

$$\rho s\Delta T = \Delta P = -\frac{8l}{r^2}\eta v_n$$

in which the viscosity coefficient η appears to be a function of temperature. This is shown in Figure 5 where we have plotted our results together with η-values determined from other experiments such as capillary flow[8,9,10], attenuation of second sound[11], and the rotating viscometer[12]. These results strongly suggest that the normal component can be considered as an ordinary viscous liquid and that the observed linear relation between $-\rho s\Delta T$ and v_n corresponds to a laminar flow of the normal component.

For the stable branch which appears at the higher values of v_n several descriptions appeared in the literature. Gorter and Mellink[5] described their observations with a cubic dependence of ΔT on $\dot{Q}$. They suggested that a mutual-

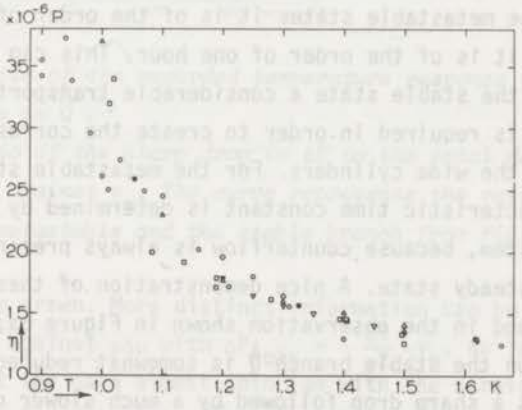

Fig. 5 *The viscosity coefficient of the normal component plotted against the temperature.*
open circles : attenuation of second sound; Zinov'eva[11].
triangles up : rotating viscometer; Woods, Heikkila and Hollis-Hallet[12].
triangles down: capillary flow; Van der Heijden, De Voogt and Kramers[8].
squares : " " ; Staas, Taconis and Van Alphen[10].
diamonds : " " ; Brewer and Edwards[9].
full circles : " " ; this research.

friction force between the superfluid and normal component proportional to the cube of the relative velocity exists in general, which in the case of pure heat flow is responsible for the observed increase in ΔT.

In Vinen's description of the flow phenomena a mutual-friction force very close to the expression of Gorter and Mellink is derived from a model in which the interaction takes place through the presence of a tangle of vortices. Vinen's own results on capillary heat flow[13] and the extensive measurements of Brewer and Edwards[6] confirmed the above description for the higher relative velocities.

It was shown by Van der Heijden et al.[1,8] that although this mutual-friction force does not give a correct description for all flow types, his data for pure heat flow could be well described in this way.

Finally Childers and Tough[14] reported recently the observation of a second critical heat input indicated by a kink in the stable branch of ΔT against $\dot{Q}$, which these authors associated with a breakdown of laminar flow of the normal-fluid component.

Before comparing our results for the stable branch with the above-mentioned observations we would like to remark that the response time of the system, i.e. the time required to reach the steady state, is quite different for the two types of flow. For the metastable states it is of the order of seconds while for the stable state it is of the order of one hour. This can be understood qualitatively as for the stable state a considerable transport of mass through the narrow capillary is required in order to create the corresponding change of the level heights in the wide cylinders. For the metastable states, on the other hand, the characteristic time constant is determined by the thermal properties of the system, because counterflow is always present even during the approach to the steady state. A nice demonstration of these two characteristic times is also found in the observation shown in Figure 6a; when starting from a steady state on the stable branch $\dot{Q}$ is somewhat reduced, the recorded response of $-\Delta T$ shows a sharp drop followed by a much slower decrease to the new steady value. In Figure 6b it is demonstrated that the sharp drops in ΔT correspond to the changes in the Poiseuille contribution to ΔT. It is the subsequent much slower decrease which restricted the measurements on the stable branch to a rather small velocity region.

As can be expected from Vinen's analysis for this velocity region[13] strong deviations from a cubic dependence of $\rho\Delta\mu$ on v_n are observed, in accordance with for instance the observations of Brewer and Edwards[6]. However, from the observed velocity dependences in this rather small transition region no definite

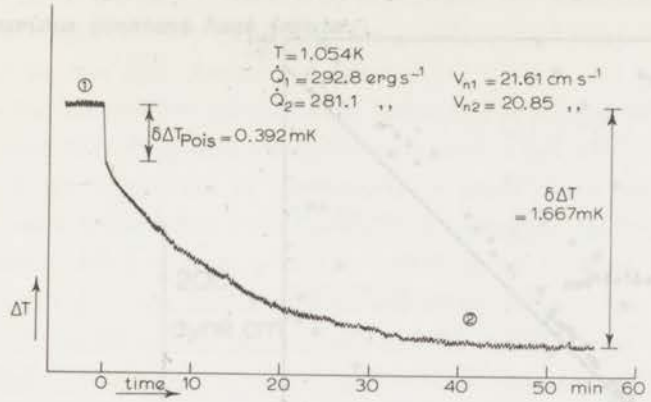

Fig. 6a

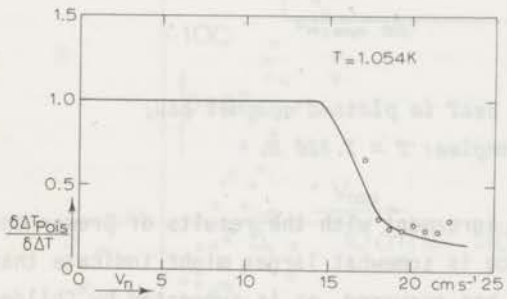

Fig. 6b

Fig. 6a *An example of the recorded temperature response to a small decrease in* $\dot{Q}$.

Fig. 6b *The ratio of the sharp drop in* ΔT *to the total decrease in* ΔT *plotted against* v_n. *The curve represents the ratio of the slopes of the metastable and the stable branch from Fig. 3b.*

conclusions can be drawn. More distinct information can be expected from a plot of $-\rho s\Delta T + \Delta P_{Pois}$ against $\rho\Delta\mu$ with $\Delta P_{Pois} = -\frac{81}{r^2}\eta v_n$, as is shown in Figure 7. From the fact that the data almost coincide with the straight line with slope one, it can be concluded that in the velocity region studied the pressure difference remains almost equal to the Poiseuille pressure difference. The small deviations at the higher values of $\rho\Delta\mu$ may not be significant, as they are very sensitive to the values for the temperature, the entropy, and the viscosity used in the calculation of the ordinate. This result could therefore be consistent with the results of Van der Heijden et al. who found that $\Delta P = \Delta P_{Pois}$. If the deviations are considered to be significant, however, it follows that the actual pressure difference becomes somewhat larger than the Poiseuille pressure

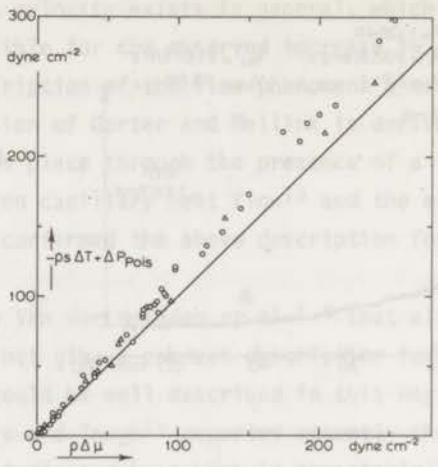

Fig. 7 *The extra contribution to ρsΔT is plotted against ρΔμ; circles: T = 1.054 K; triangles: T = 1.326 K.*

difference, which is in qualitative agreement with the results of Brewer and Edwards. That the pressure difference is somewhat larger might indicate that a change in the normal-flow behaviour has occurred, as is suggested by Childers and Tough.

As the present apparatus was designed to study the flow at low velocities, conclusive evidence that would follow from a study at high velocities cannot be given.

3.3 Combined flow

Two series of measuring runs can be distinguished. One in which at a number of fixed heat inputs $\dot{Q}$, ΔT and ΔZ were measured as a function of the plunger speed v_p. The velocity region $10^{-3} < |v_p| < 10^{-2}$ cm s^{-1} corresponds to a mass-flow velocity in the capillary v_{cap} up to several cm s^{-1} in both directions. The second in which at fixed values of the plunger speed v_p the heat input $\dot{Q}$ was varied corresponding to a normal flow velocity up to 20 cm s^{-1} always in the positive direction. The results of both series prove to be equivalent showing that the steady-state results are independent of the order in which the two external parameters are adjusted.

Figures 8a and b show $\rho s \Delta T$ against v_{cap} at fixed values of $\dot{Q}$ for the two bath temperatures. Figures 9a and b show the corresponding results for $\rho \Delta \mu$.

The results for ρsΔT and ρΔμ at T = 1.326 K as a function of the mass flow at various constant heat inputs.

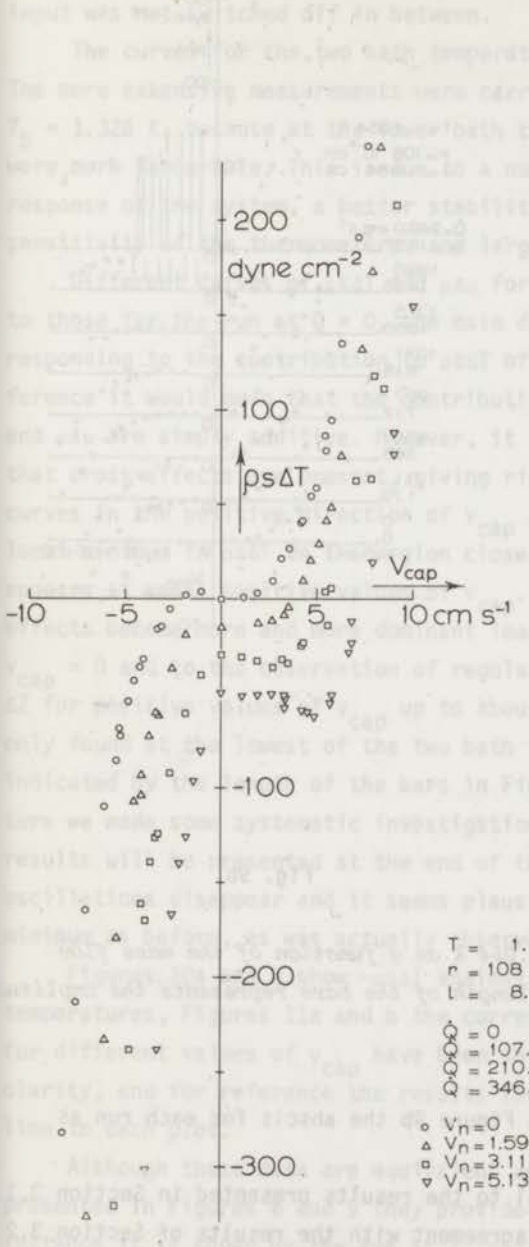

Fig. 8a

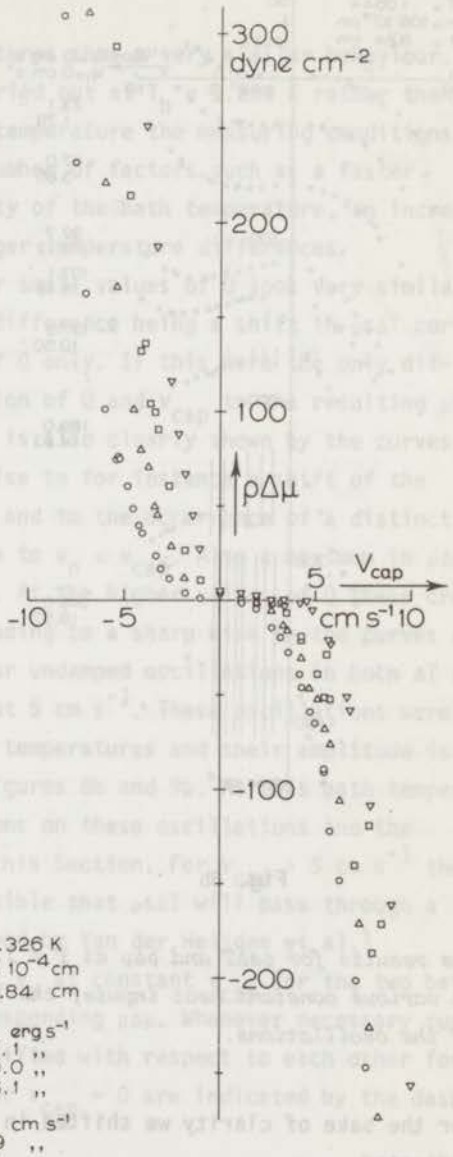

Fig. 9a

T = 1.326 K
r = 108 10^{-4} cm
l = 8.84 cm

$\dot{Q}$ = 0 erg s⁻¹
$\dot{Q}$ = 107.1 ,,
$\dot{Q}$ = 210.0 ,,
$\dot{Q}$ = 346.1 ,,

○ V_n = 0 cm s⁻¹
△ V_n = 1.59 ,,
□ V_n = 3.11 ,,
▽ V_n = 5.13 ,,

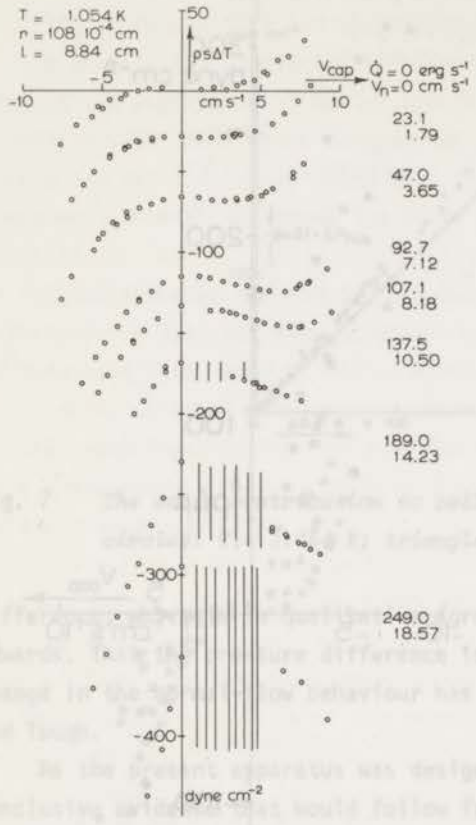

Fig. 8b

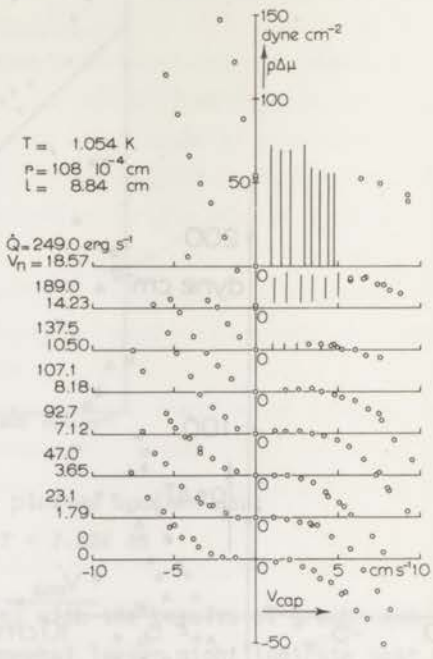

Fig. 9b

The results for ρsΔT and ρΔμ at T = 1.054 K as a function of the mass flow at various constant heat inputs; the length of the bars represents the amplitude of the oscillations.

For the sake of clarity we shifted in Figure 9b the abscis for each run as indicated.

The runs with $\dot{Q} = 0$ are identical to the results presented in Section 3.1. The data on the $v_{cap} = 0$ axes are in agreement with the results of Section 3.2 within the measuring accuracy of a few percent. Only for the highest value of $\dot{Q} = 249.0$ erg s^{-1} and $T_b = 1.054$ K two points for $v_{cap} = 0$ were found, the lowest corresponding to the metastable branch, the other to the stable one of

Figures 3b and 4b. It should be mentioned that once the plungers were set in motion, usually only points on the stable branch were found as long as the heat input was not switched off in between.

The curves for the two bath temperatures show a very similar behaviour. The more extensive measurements were carried out at T_b = 1.054 K rather than at T_b = 1.326 K, because at the lower bath temperature the measuring conditions were more favourable. This is due to a number of factors such as a faster response of the system, a better stability of the bath temperature, an increased sensitivity of the thermometers, and larger temperature differences.

Different curves of $\rho s\Delta T$ and $\rho\Delta\mu$ for small values of $\dot{Q}$ look very similar to those for the run at $\dot{Q} = 0$, the main difference being a shift in $\rho s\Delta T$ corresponding to the contribution to $\rho s\Delta T$ of $\dot{Q}$ only. If this were the only difference it would mean that the contribution of $\dot{Q}$ and v_{cap} to the resulting $\rho s\Delta T$ and $\rho\Delta\mu$ are simply additive. However, it is also clearly shown by the curves that cross-effects are present, giving rise to for instance a shift of the curves in the positive direction of v_{cap} and to the occurrence of a distinct local minimum in $\rho s\Delta T$ in the region close to $v_n \approx v_{cap}$. Also a maximum in $\rho\Delta\mu$ appears at small positive values of v_{cap}. At the higher values of $\dot{Q}$ these cross-effects become more and more dominant leading to a sharp kink in the curves at $v_{cap} = 0$ and to the observation of regular undamped oscillations in both ΔT and ΔZ for positive values of v_{cap} up to about 5 cm s^{-1}. These oscillations were only found at the lowest of the two bath temperatures and their amplitude is indicated by the length of the bars in Figures 8b and 9b. At this bath temperature we made some systematic investigations on these oscillations and the results will be presented at the end of this Section. For $v_{cap} > 5$ cm s^{-1} the oscillations disappear and it seems plausible that $\rho s\Delta T$ will pass through a minimum as before, as was actually observed by Van der Heijden et al.[1]

Figures 10a and b show $-\rho s\Delta T$ against v_n at constant v_{cap} for the two bath temperatures, Figures 11a and b the corresponding $\rho\Delta\mu$. Whenever necessary curves for different values of v_{cap} have been shifted with respect to each other for clarity, and for reference the results for $v_{cap} = 0$ are indicated by the dashed line in each plot.

Although these data are equivalent and in numerical agreement with those presented in Figures 8 and 9 they provide some additional information. For instance it is shown by the run at T_b = 1.326 K and v_{cap} = 1.10 cm s^{-1} in Figure 10a that not only for $v_{cap} = 0$ but also for small $|v_{cap}|$ metastability can be observed. Furthermore, many of the data shown in Figures 10 and 11 correspond to rather small values of $\rho\Delta\mu$ because v_{cap} is rather small. For these

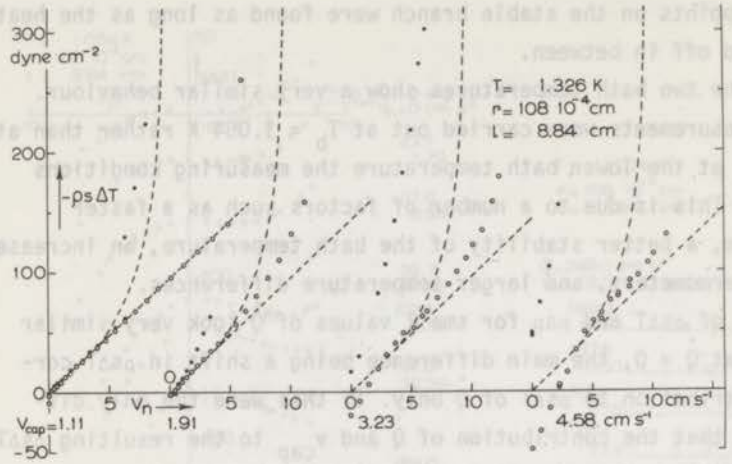

Fig. 10a

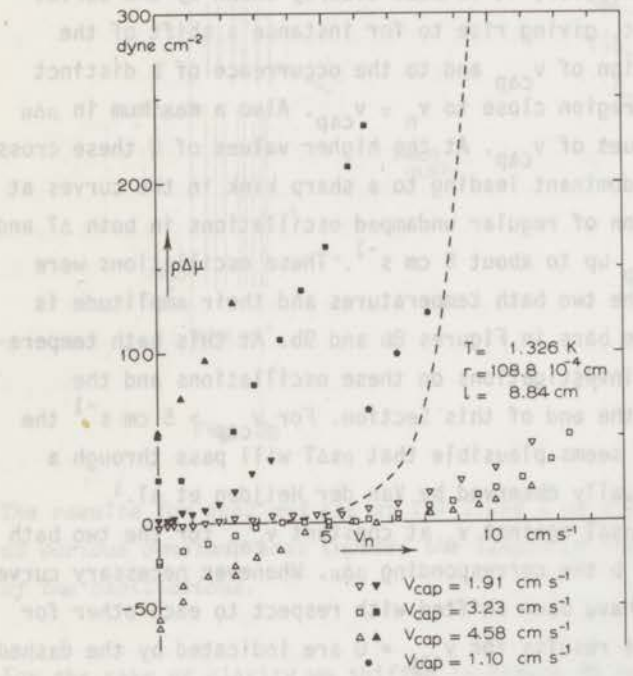

Fig. 11a

The results for $-\rho s\Delta T$ and $\rho\Delta\mu$ at T = 1.326 K as a function of the heat input at various constant values of the mass flow; the open (full) symbols represent mass flow in the positive (negative) direction; for the run at $|v_{cap}|$ = 1.10 cm s^{-1} only the data for which $\rho\Delta\mu \neq 0$ are shown. The dashed lines represent the results for $v_{cap} = 0$.

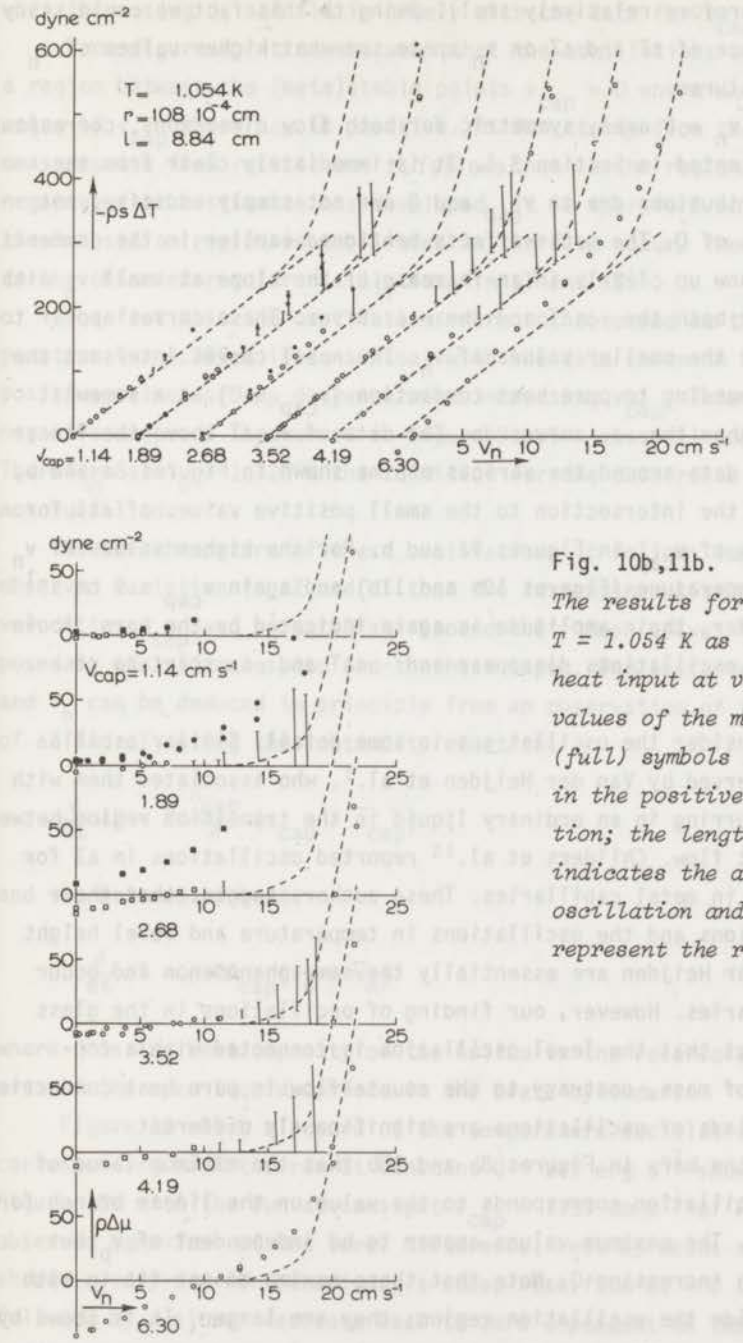

Fig. 10b,11b.

The results for $-\rho s\Delta T$ and $\rho\Delta\mu$ at $T = 1.054$ K as a function of the heat input at various constant values of the mass flow; the open (full) symbols represent mass flow in the positive (negative) direction; the length of the bars indicates the amplitude of the oscillation and the dashed lines represent the results for $v_{cap} = 0$.

data the response time of the system is primarily determined by its thermal properties and is therefore relatively small. Owing to this fact we could study the velocity dependence of ΔT and ΔZ on v_n up to somewhat higher values of v_n for both bath temperatures.

The data on the $v_n = 0$ axes, symmetric for both flow directions, correspond again with those presented in Section 3.1. It is immediately clear from the curves that the contributions due to v_{cap} and $\dot{Q}$ are not simply additive, not even for small values of $\dot{Q}$. The cross-effects mentioned earlier in the comments on Figures 8 and 9 show up clearly in an increase of the slope at small v_n with increasing $|v_{cap}|$ for both the $-\rho s\Delta T$ and the $\rho\Delta\mu$ curves. These curves appear to be straight lines for the smaller values of v_n. The $-\rho s\Delta T$ curves intersect the linear branch corresponding to pure heat conduction ($v_{cap} = 0$) at a somewhat smaller value of v_n than the $\rho\Delta\mu$ curves do. The data of $-\rho s\Delta T$ above the linear branch correspond to data around the various minima shown in Figures 8a and b, the data of $\rho\Delta\mu$ past the intersection to the small positive values of $\rho\Delta\mu$ for small positive values of v_{cap} in Figures 9a and b. For the higher values of v_n at the lower bath temperature (Figures 10b and 11b) and again $v_{cap} \lesssim 5$ cm s^{-1} the oscillations appear, their amplitude is again indicated by the bars. Above $v_n \sim 20$ cm s^{-1} these oscillations disappear and $-\rho s\Delta T$ and $\rho\Delta\mu$ start to rise steeply.

We will here consider the oscillations in some detail. Similar oscillations were first observed by Van der Heijden et al.[1], who associated them with the oscillations occurring in an ordinary liquid in the transition region between laminar and turbulent flow. Childers et al.[15] reported oscillations in ΔT for pure heat conduction in metal capillaries. These authors suggest that their temperature oscillations and the oscillations in temperature and level height as observed by Van der Heijden are essentially the same phenomenon and occur only in metal capillaries. However, our finding of oscillations in the glass capillary and the fact that the level oscillation is connected with a considerable transport of mass, contrary to the counterflow in pure heat conduction, prove that the two kinds of oscillations are significantly different.

It is shown by the bars in Figures 8b and 10b that the minimum value of $|\rho s\Delta T|$ during the oscillation corresponds to the value on the linear branch for pure heat conduction. The maximum values appear to be independent of v_p but increase clearly with increasing $\dot{Q}$. Note that these maxima do not fit in with the $\rho s\Delta T$ values outside the oscillation region; they are larger. It is shown by the bars in Figures 9b and 11b that the minimum value of $\rho\Delta\mu$ during the oscillation also corresponds to the value on the linear branch for pure heat

conduction, i.e. $\rho\Delta\mu = 0$. The maxima of $\rho\Delta\mu$ are also independent of v_p, increase with increasing $\dot{Q}$, and fit in nicely with the data for $v_{cap} \geq 5\ cm\ s^{-1}$.

From figure 9b it can be seen that the oscillations at constant $\dot{Q}$ occur in a region between the (meta)stable points $v_{cap} = 0$ where $\rho\Delta\mu = 0$ and a positive value of v_{cap} where $\rho\Delta\mu$ is positive. As for steady flow the level difference measures the flow resistance, it follows that in the region of oscillations a negative flow resistance has developed. It is therefore not surprising that in the transition region instabilities in the flow occur. These instabilities lead to the observed regular oscillations in ΔT and ΔZ[16].

The fact that the oscillations were not observed at the higher bath temperature T = 1.326 K is consistent with the data shown in Figure 11a, where the positive values of $\rho\Delta\mu$ decrease with increasing v_{cap}. This corresponds to a negative slope of the curves in Figure 9a also at small positive values of v_{cap}. Therefore at $T_b = 1.326$ K the condition for the occurrence of instabilities is not fulfilled.

As for the nature of these oscillations it follows immediately from the observed variation in ΔZ and ΔT that the instantaneous values of the transport velocities v_{cap} and v_n oscillate around their mean values $\overline{v}_{cap}$ and $\overline{v}_n$ as imposed by the plunger speed and the heat input. The instantaneous values of v_{cap} and v_n can be deduced in principle from an observation of the time dependence of ΔZ and ΔT, using the continuity equation:

$$\frac{d}{dt}\Delta Z = 2\frac{A_{cap}}{A}(v_{cap} - \overline{v}_{cap}) \quad , \qquad (a)$$

and the balance of heat:

$$C\frac{d}{dt}\Delta T = \rho s T A_{cap}(v_n - \overline{v}_n) \qquad (b)$$

where C is the heat capacity of the helium in the reservoir at T_1 and A the area of the open liquid surface in the brass cylinders.

Figure 12 shows a record of the temperature oscillations, Figure 12a corresponding with the run at constant $\dot{Q} = 249\ erg\ s^{-1}$ shown in Figure 8b, and Figure 12b with the run at constant $v_{cap} = 1.89\ cm\ s^{-1}$ of Figure 10b. The observed behaviour of the level difference, read by means of a cathetometer, showed a very similar behaviour: a steep rise from $\Delta Z = 0$ to its maximum value followed by a slower decrease back to zero dependent on the value of $\overline{v}_{cap}$ in a similar fashion as displayed by the ΔT oscillations in Figure 12. The minima in ΔZ and $-\Delta T$ were reached almost simultaneously, in the maxima ΔZ was sometimes

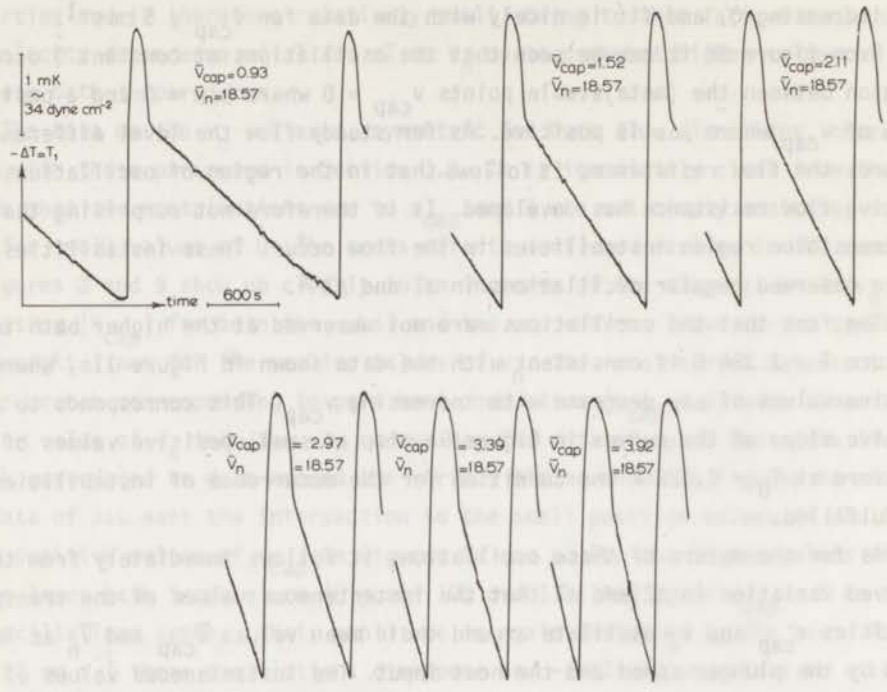

Fig. 12a

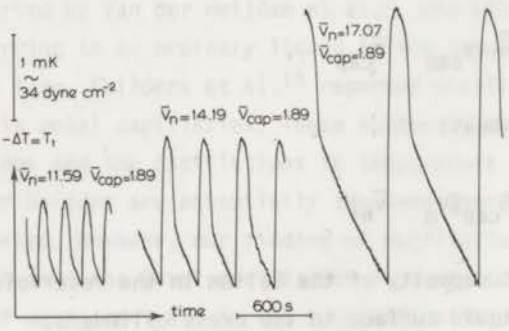

Fig. 12b

Fig. 12a,b *Two examples of the temperature oscillations. Fig. 12a shows ΔT for different values of $\bar{v}_{cap}$ at constant $\bar{v}_n$; Fig. 12b shows ΔT for different values of $\bar{v}_n$ at constant $\bar{v}_{cap}$.*

observed to lag behind. According to equation (a) the steep increase in ΔZ corresponds to a flow velocity v_{cap} which is much larger than $\bar{v}_{cap}$, while during the decrease back to zero v_{cap} is obviously smaller than $\bar{v}_{cap}$. Figure 13 shows a schematic diagram of the hysteretic loop which corresponds to this time behaviour of ΔZ. A rough estimate of the flow velocity v_{cap} from the available data of $\Delta Z(t)$ suggests strongly that the branches 2 and 4 in Figure 13 correspond to the branches for steady flow in Figure 9b outside the unstable region. This seems plausible, because the inertial forces due to the acceleration and deceleration of the flow remain small on these branches as can be estimated using equation (a) from the observed averaged slopes of $\Delta Z(t)$. It is also in accordance with the observation that the maxima in $\rho\Delta\mu$ fit in nicely with the data for steady flow beyond the unstable region in Figure 9b. The branches 1 and 3, crossing the unstable region, correspond to a rapid acceleration respectively deceleration of the flow occurring in a small time interval at the minimum respectively maximum of $\rho\Delta\mu$.

It should be noted that during the hysteretic loop the value of v_n is not constant. The decrease of v_n during the initial steep increase of $-\Delta T$ in Figure 12 which corresponds to the branches 1 and 2 of the hysteretic loop in Figure 13, can be estimated from equation (b) using the calculated heat capacity of the helium in the reservoir $C = 2.5 \times 10^5$ erg K^{-1}. It is found that this decrease never exceeds 20% of $\bar{v}_n$. The final slopes in Figure 12a, corresponding to branch 4 in Figure 13 are plotted in Figure 14 as a function of $\bar{v}_{cap}$. On the ordinate on the right the corresponding increments in v_n are indicated showing that v_n never exceeds $\bar{v}_n = 18.57$ cm s^{-1} by more than 1%.

If branch 4 of the hysteretic loop does indeed correspond to the stable branch for $v_{cap} < 0$ of Figures 8b and 9b, the values of $-\frac{d}{dt}\rho\Delta\mu$ and $\frac{d}{dt}\rho s\Delta T$ should be almost equal because their sum equals $-\frac{d}{dt}\Delta P$. From a numerical

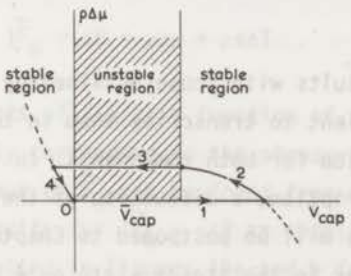

Fig. 13
Schematic diagram of the hysteretic loop during an oscillation.

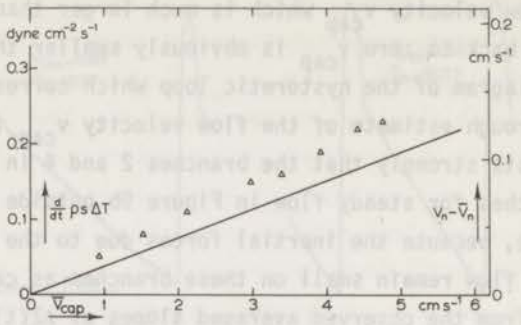

Fig. 14 *The final slopes of* $\rho s\Delta T$ *from Fig. 12a as a function of* $\bar{v}_{cap}$. *The drawn line corresponds to* $-\frac{d}{dt}\rho\Delta\mu$, *calculated from equation (a) for* $v_{cap} = 0$.

comparison of the data for $\rho s\Delta T$ in Figure 8b with those for $\rho\Delta\mu$ in Figure 9b it appears that $\Delta P \simeq \Delta P_{Pois}$ on the stable branch, so that indeed $\frac{d}{dt}\Delta P \simeq 0$. This suggestion is confirmed by the fact that the observed maximum values of $\rho\Delta\mu$ as given in Figure 9b are almost equal to the corresponding differences in $-\rho s\Delta T$ for the linear decrease in Figure 12. The drawn line in Figure 14 shows $-\frac{d}{dt}\rho\Delta\mu$ calculated from equation (a) for the case that $v_{cap} = 0$. Comparison with the data shows that during branch 4 of the hysteretic loop, v_{cap} remains close to zero; from the deviation it is suggested that perhaps a small negative value of v_{cap} is present.

From the above arguments we conclude that the oscillations can be explained in terms of the behaviour during steady flow. For a precise quantitative verification of this conclusion accurate and simultaneous measurements of ΔZ and ΔT as a function of time are required.

4. Discussion of the results

In order to compare the experimental results with those obtained by others in different experiments, it is often convenient to transcribe them in terms of the forces appearing in the equations of motion for both components. In this Section we will merely carry out this transcription, a discussion of the hydrodynamic processes responsible for the results will be postponed to Chapter IV. It is sufficient to mention here that whenever in the steady state $\Delta\mu \neq 0$ a directed motion of superfluid vortex lines takes place throughout the flow path. It is this vortex process which leads to the observed phenomena.

The equations of motion for the transport velocities in the capillary can be written as:

$$\rho_s \frac{\partial v_s}{\partial t} = - \rho_s \frac{d\mu}{dx} - F_{sn} \qquad (1)$$

$$\rho_n \frac{\partial v_n}{\partial t} = - \rho_n \frac{d\mu}{dx} - \rho s \frac{dT}{dx} + F_{sn} - F_n \quad . \qquad (2)$$

These equations are slightly different from those presented in Chapter I, the main difference being that F_s, appearing in Chapter I, has been set equal to zero. As has been stated in the General Introduction one assumption about the forces F_s, F_{sn}, and F_n has to be made in order to deduce their values from the experimental results on $\Delta\mu$ and ΔT. In Chapter I it seemed plausible to assume $F_n \approx 0$ when $v_n \approx 0$ during the experiment, which led directly to the occurrence of a force F_s suggesting a direct transfer of momentum from the superfluid to the wall of the capillary. However, as it seems inconceivable for such a direct transfer to occur we prefer here to impose $F_s = 0$, implying that F_n can be unequal to zero even when $v_n = 0$. The equations written in this way thus suggest that the superfluid can only exchange momentum with the normal component through the mutual interaction F_{sn}. Part of this momentum is then transferred to the wall by the viscosity of the normal component, not only due to the normal transport but also due to a circulation, a turbulence of the normal component introduced by the interaction. In this way of writing the equations F_s of Chapter I is simply included in F_n, while $F_{sn} + F_s$ in Chapter I corresponds to F_{sn} in the notation of this Chapter.

Integration of equations (1) and (2) along the capillary renders immediately for the forces F_{sn} and F_n, averaged over the capillary

$$- l\overline{F}_{sn} = \rho_s \Delta\mu \qquad (3)$$

$$- l\overline{F}_n = \Delta P = \rho\Delta\mu + \rho s \Delta T \quad . \qquad (4)$$

The plots of $\rho\Delta\mu$ as a function of v_n and v_{cap}, as given in Section 3, therefore directly correspond to the steady-state behaviour of $- \frac{\rho}{\rho_s} l\overline{F}_{sn}$, while the behaviour of $\overline{F}_n$ can be found from an addition of the results for $\rho\Delta\mu$ and $\rho s\Delta T$. The results for $l\overline{F}_n = -\Delta P$ as obtained for the series at constant v_n of Section 3, are plotted in Figures 15a and b for the two bath temperatures. From these plots it follows that deviations from the Poiseuille law occur, the deviations being almost independent of the bath temperature as was also found in Chapter I. It

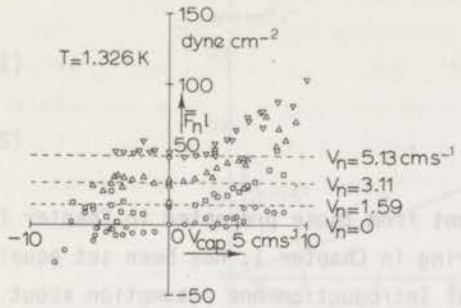

Fig. 15a

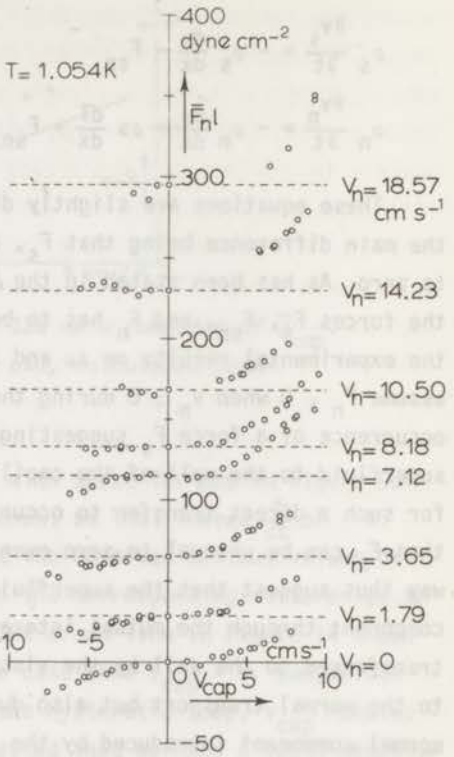

Fig. 15b

Fig. 15a,b $\overline{F}_n l$ *as a function of* v_{cap} *at constant values of* v_n*, showing the deviation from Poiseuille's law; the latter contribution to* $\overline{F}_n l$ *is represented by the dashed lines for each run.*

should be mentioned that the cubic dependence of F_s on v_{cap} suggested from the data on $v_n = 0$ flow in Chapter I must clearly be considered as a simplification. The data of F_n for $v_n \neq 0$, presented in Figures 15a and b show that its behaviour is more complicated.

We conclude that the qualitative behaviour of $\overline{F}_{sn}(v_s, v_n)$ and $\overline{F}_n(v_s, v_n)$ as deduced from the present investigation is representative for the steady-state behaviour of these quantities in a wide range of flow experiments. This conclusion is based on the close agreement in the experimental results that appeared in the literature, though this agreement is often obscured by the differences in their interpretation. For instance, the general results on capillary flow as reported by Van der Heijden et al.[1] and by Van Alphen et al.[17], and the

results on pure heat conduction as reported by Brewer and Edwards[6] and by Tough et al.[14] are in good qualitative agreement with the present observations. Perhaps the strongest evidence for the above conclusion is the fact that oscillations in the flow reported in Section 3 were also found in the experiments of Van der Heijden et al. As the occurrence of these oscillations can be attributed to the presence of a small positive maximum in $-\overline{F}_{sn}$, it follows that this behaviour of $\overline{F}_{sn}$ must be a general property of the flow.

It now remains to find the dynamic processes responsible for the observed steady-state behaviour. More direct information about these processes could be obtained from a knowledge of the time development of the observable quantities to their steady values for given constant values of v_n and v_s. However, the present experiments on the steady-flow behaviour are not very suitable to obtain this information. The intrinsic time constant of the dynamic process is obscured by the large time constants of the apparatus, i.e. the thermal relaxation time and the time required by the mass transport through the narrow capillary to build up the steady value of $\Delta\mu$. It seems hardly possible to separate the different contributions from the total response time of the system and we therefore did not attempt to analyse the recorded growth and decay of for instance the temperature difference at a given pre-set value of the heat input and the plunger speed. Moreover, we have some evidence to believe that in the investigated temperature and velocity region the intrinsic time constant is small compared to those of the apparatus. Perhaps the clearest evidence follows from the following observation. When during the experiments presented in Figures 8 and 9 at a given value of the heat input the plungers were set into motion with a speed corresponding to a positive v_{cap} larger than that of the minimum in ΔT (Figure 8), it was observed that the recorder trace of ΔT also passed through the minimum before reaching its higher steady value. Obviously the intrinsic time required by the dynamic process to reach its steady state is smaller than the time required by the velocities to reach their steady values.

It should be remarked that, for simplicity, such a small intrinsic time constant was implicitly assumed in the description of the observed oscillations in the flow, given in Section 3. A clear indication that this assumption is justified is found in the fact, mentioned earlier, that the maxima in $\rho\Delta\mu$ during the oscillation were found to fit in smoothly with the steady values of $\rho\Delta\mu$ outside the oscillating region. The intrinsic time constant is therefore small, at least on the time scale of the oscillation.

Although it might be possible to obtain an estimate on the time constant from carefully designed flow experiments (in general the study of the properties

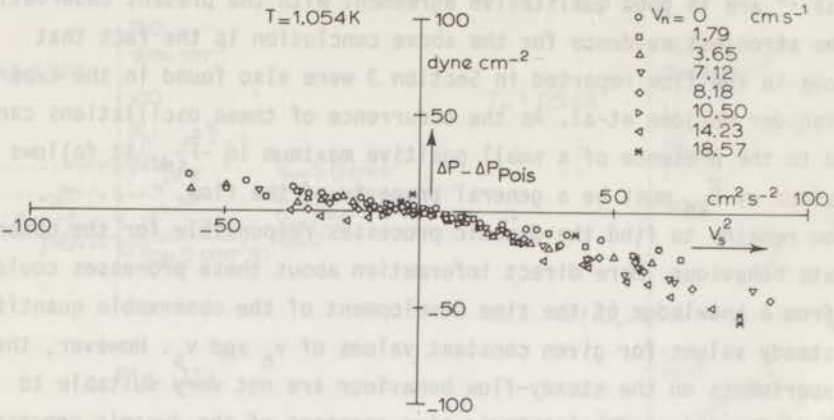

Fig. 16a *The extra pressure difference over the capillary as a function of v_s^2 for different values of v_n; the positive (negative) abscis indicates the positive (negative) direction of the superfluid transport.*

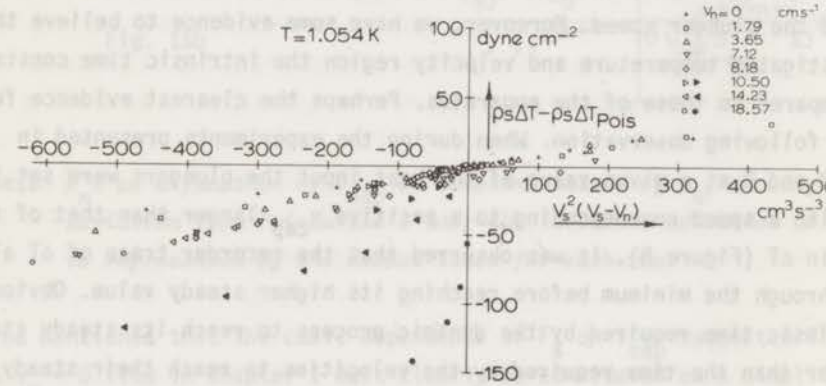

Fig. 16b *The extra temperature difference over the capillary as a function of $v_s^2(v_s - v_n)$ for different values of v_n; the full symbols correspond to the negative direction of the superfluid flow at large values of v_n.*

of second sound seems a better tool), the present experiments did not provide this information.

For a comparison of different flow experiments it would be convenient to find analytic expressions for $\overline{F}_n(v_n,v_s)$ and $\overline{F}_{sn}(v_n,v_s)$, though these expressions may turn out to be misleading. In Chapter I we verified that, at least when $v_n \approx 0$, $\overline{F}_{sn}$ and $\overline{F}_n$ are independent of the length and type of capillary used. The information on the dependence on the diameter of the capillary is less clear. However, apart from the deviating behaviour of the 340 micron stainless-steel capillary mentioned in Chapter I, a comparison of the results obtained in different capillaries (for instance on pure heat conduction or Van der Heijden's results on general flow) with the present results shows that $\overline{F}_{sn}$ is not very sensitive to a change in diameter, at least in the range of a few hundred microns.

We did not succeed in finding a good analytic expression for $\overline{F}_{sn}$ and $\overline{F}_n$ that covered all the results. The best attempt is perhaps:

$$\overline{F}_n = \frac{32\eta}{d^2} v_n + B|v_s|v_s \qquad (5)$$

$$\overline{F}_{sn} = A\rho_s\rho_n v_s^2(v_s - v_n - v_o) + B\frac{\rho_s}{\rho}|v_s|v_s \quad . \qquad (6)$$

The adjustable parameters A, v_o, and B are such that A corresponds to a Gorter-Mellink or Vinen type of constant, presented in Figure 5 of Chapter I, v_o is in the order of 1 cm s^{-1} and varies slightly with v_n (e.g. $v_o = 0$ if $v_n = 0$), and the constant B (≈ 0.04 g cm^{-4}) is almost independent of T. From the equations of motion it follows that

$$\Delta P = \Delta P_{Pois} - Bl|v_s|v_s$$

$$\rho s\Delta T = \rho s\Delta T_{Pois} + Al\rho\rho_n v_s^2(v_s - v_n - v_o) \quad .$$

In Figure 16a $\Delta P - \Delta P_{Pois}$ is plotted against v_s^2 for $T_b = 1.054$ K, Figure 16b shows $\rho s\Delta T - \rho s\Delta T_{Pois}$ against $v_s^2(v_s - v_n)$, both plots contain the data of the runs at constant v_n. As one can see from these plots the fit is rather poor but the expressions (5) and (6) demonstrate some of the characteristic features of the observed quantities. They describe satisfactorily the flow with $v_n = 0$, where $\rho s\Delta T$ is found to have a cubic dependence on v_s (Chapter I), while for $v_n > 0$ a region in which $\rho\Delta\mu$ is positive appears between $v_{cap} \approx v_s \approx 0$ and $v_{cap} \approx v_s \approx v_n + v_o - \frac{B}{A\rho\rho_n}$. Also $\rho s\Delta T$ shows a minimum where

$$v_s = \frac{2}{3}(v_n + v_o) > \frac{2}{3}(v_n + v_o - \frac{B}{A\rho\rho_n}) \quad ,$$

the latter being the position of the maximum in $\rho\Delta\mu$. However, they do not account for, for instance, the deviating behaviour of $\rho s\Delta T$ for large values of v_n and negative values of v_{cap} shown in Figure 16b, nor do they describe the sharp rise in $\Delta\mu$ found for pure heat conduction (Figures 4a and 4b), giving rise to the disappearance of the maximum in $\rho\Delta\mu$ at higher v_n. Perhaps this latter contribution to $\overline{F}_{sn}$, which should be included in equation (6), can also account for the fact that at T = 1.326 K such a maximum does not show up at all.

It did not seem worthwhile to spend more effort in adding more adjustable parameters to the equations (5) and (6) in order to get a better analytic fit to the data. In the above discussion most of the remarkable properties of the forces have shown up.

It seems surprising that the mutual interaction between the superfluid and normal component appears to depend on the individual transport velocities with respect to the wall of the capillary and not only on the relative velocity $v_s - v_n$, and that $\overline{F}_{sn}$ does not even contain a factor $v_s - v_n$ so that, when both components move with the same transport velocity, their mutual interaction does not equal zero. Obviously such properties cannot be understood in terms of the transport velocities alone. For the understanding a local description is required as the observed quantities result from the local dynamic processes taking place in the capillary.

It should be remarked that F_{sn} does not contribute to the entropy production in the steady state when the transport velocities are equal. This is true as the entropy production in the steady state can be written as*:

$$\frac{\Sigma}{T} = \frac{F_{sn}(v_s - v_n) + F_n v_n}{T} \quad . \qquad (7)$$

Equation (7) can be derived from the equations of motion (1) and (2) using the expression for the energy dissipation

---

* It should be mentioned that a proper treatment of the entropy production should be based on the dissipative equations of Khalatnikov. The above calculation is based on the transport equations (1) and (2), that can be considered as a convenient substitute for a comparison with the experiments, as only the transport velocities are always determined experimentally.

$$\dot{\Delta q} = -\rho v \Delta\mu \qquad (8)$$

in which $\dot{q}$ is the heat-flux density

$$\dot{q} = \rho s T v_n \quad . \qquad (9)$$

Namely, rewriting equation (7):

$$\frac{F_{sn}(v_s - v_n) + F_n v_n}{T} = \frac{-\rho v \frac{d\mu}{dx} - \rho s v_n \frac{dT}{dx}}{T} = \frac{d}{dx} \rho s v_n = \frac{\Sigma}{T} \quad . \qquad (10)$$

One has to conclude that the vortex process responsible for the occurrence of the mutual interaction is still maintained ($F_{sn} \neq 0$), even when the transport velocities i.e. the local velocities averaged over time and cross-section, are equal ($v_s - v_n = 0$).

We use this opportunity to remark that it follows from equation (8) that for pure heat conduction ($\rho v = 0$), the energy dissipation is always zero even on the steeper branch where $\Delta\mu \neq 0$, but that the entropy production according to equation (10) is what it should be[18].

References

1. Van der Heijden, G., Van der Boog, A.G.M. and Kramers, H.C., Physica 77 (1974) 487 (Commun., Leiden, No. 411c).
2. Olijhoek, J.F., Van Beelen, H., De Bruyn Ouboter, R., Taconis, K.W. and Koops, W., Physica 72 (1974) 355 (Commun., Leiden, No. 406a).
3. Staas, F.A. and Severijns, A.P., Cryogenics 9 (1969) 422.
4. Olijhoek, J.F., Hoffer, J.K., Van Beelen, H., De Bruyn Ouboter, R. and Taconis, K.W., Physica 64 (1973) 289 (Commun., Leiden, No. 399b).
5. Gorter, C.J. and Mellink, J.H., Physica 15 (1949) 285 (Commun., Leiden, Suppl. No. 98a) and references therein.
6. Brewer, D.F. and Edwards, D.O., Phil. Mag. 7 (1962) 721, and references therein.
7. Chase, C.E., Phys. Rev. 127 (1962) 361.
8. Van der Heijden, G., De Voogt, W.J.P. and Kramers, H.C., Physica 59 (1972) 473 (Commun., Leiden, No. 392a).
9. Brewer, D.F. and Edwards, D.O., Proc. Roy. Soc. A251 (1959) 247.

10. Staas, F.A., Taconis, K.W. and Van Alphen, W.M., Physica 27 (1961) 893 (Commun., Leiden, No. 328d).
11. Zinov'eva, K.N., Sov. Phys. JETP 4 (1957) 36.
12. Woods, A.D.B. and Hollis-Hallet, A.C., Can. J. Phys. 41 (1963) 596. Heikkila, W.J. and Hollis-Hallet, A.C., Can. J. Phys. 33 (1955) 420.
13. Vinen, W.F., Proc. Roy. Soc. 243 (1958) 400 and references therein.
14. Childers, R.K. and Tough, J.T., Phys. Rev. Lett. 31 (1973) 911; 35 (1975) 527.
15. Childers, R.K. and Tough, J.T., J. low Temp. Phys. 15 (1974) 63.
16. De Haas, W. and Van Beelen, H., Proc. XIV Int. Conf. low Temp. Phys., Otaniemi, Finland 1 (1975) 215.
17. Van Alphen, W.M., De Bruyn Ouboter, R. and Taconis, K.W., Physica 44 (1969) 51 (Commun., Leiden, No. 371a).
18. Oliphant, T.R., Annals of Phys. 23 (1963) 38.

CHAPTER III

SUPERFLUID AND NORMAL FLOW UNDER THE CONDITION $\Delta\mu = 0$

Synopsis

The results of experiments in which $\Delta\mu = 0$ for steady flow is realized by generating the flow in a closed circuit, are compared with the results for general flow presented in Chapter II. In addition to the agreement found between the two experiments, the conservation of circulation is discussed in detail. A comparison is made between flow with $\Delta\mu = 0$ and pure heat conduction.

1. Introduction

In this Chapter measurements will be discussed on adiabatic flow through a capillary which together with a superleak forms a closed flow circuit. One connection between the capillary and the superleak is in direct thermal contact with the bath. In the other connection the flow is generated by means of a heater. As $\Delta\mu$ over the superleak is zero steady flow through the capillary must obey the stringent condition $\Delta\mu_{cap} = 0$.

This interesting type of flow was first studied by Staas, Taconis, and Van Alphen[1]. They argued that in order to obey the condition $\Delta\mu_{cap} = 0$ the occurrence of an effective mutual friction should be avoided. This is accomplished by a supply of superfluid through the superleak. This type of flow is thus quite different from that in the usual heat conduction experiments where large relative velocities are present due to the superfluid counterflow.

Their experimental results showed two distinct flow regimes: up to a critical heat input the dependence of ΔT and ΔP on the normal velocity obeyed Poiseuille's law. Above the critical heat input the Poiseuille branch became metastable and a new stable branch was observed analogous to that of Blasius flow of an ordinary fluid, as the temperature and the pressure difference were found to vary with a 1.75 power of v_n. The critical heat input described with

a Reynolds number $\rho v_n d\eta^{-1}$ occurred at a value $\sim$ 1200. These observations led Staas et al. to the conclusion that the liquid moves as a whole ($v_n = v_s = v$) like an ordinary liquid, and that the interaction with the wall occurs through its viscosity which is equal to the viscosity of the normal component.

A different interpretation was given by Van der Heijden, Van der Boog, and Kramers[2]. In their picture the condition $\Delta\mu = 0$ is fulfilled by allowing for a superfluid friction F_s balancing the mutual friction F_{sn}. The superfluid friction F_s accounts for an extra momentum transfer to the wall.

They were led to this interpretation by their experimental results on this type of flow in combination with their results for flow with independently adjustable v_n and v_s. These latter results suggested that the normal flow remained laminar while the superfluid flow resembled strongly that of an ordinary liquid, a laminar region followed by a turbulent (Blasius) type of flow. Both fluids interact with each other through a mutual friction F_{sn}. From these measurements it was found that $\rho\Delta\mu = 0$ when $v_s \approx 0$ as well as when $v_s \approx (v_n - 2)\text{cm s}^{-1}$. They identified their results on what they called "non-restricted superfluid flow" with the latter results and found a good agreement between their experimental data, which were slightly different from those found by Staas et al.

Before the results of the measurements described in Chapter II were obtained a new investigation on $\Delta\mu = 0$ flow was started in order to judge the validity of either of the two descriptions. Neither of them seems to us fully acceptable. The description of Staas et al., where the two fluids lock into each other, is incompatible with the experiments at independently adjustable v_n and v_s, though it does not need the inconceivable assumption of a direct interaction of the superfluid with the wall as is suggested in the description of Van der Heijden et al. The merit of the latter description is that in their interpretation the $\Delta\mu = 0$ flow can be understood in terms of the general flow behaviour.

Section 2 gives a description of the apparatus, Section 3 the experimental results. In Section 4 a discussion is presented of the results in connection with the findings of Chapter II.

2. Experimental set-up

Figure 1 shows a schematic drawing of the apparatus. In the vacuum can the superleak S and the glass capillary C are connected to each other via stainless-steel and glass tubes of i.d. 0.25 cm. The carbonthermometers T_1 and T_2 and the

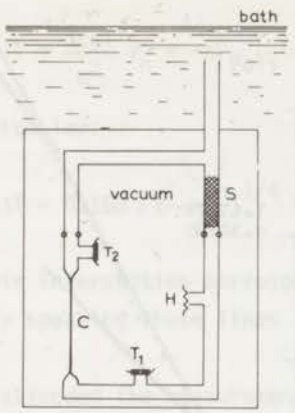

Fig. 1 *Schematic drawing of the apparatus. C: capillary; S: superleak; H: heater; T: carbon thermometer.*

heater H were mounted on small copper plugs which were in direct contact with the helium through the glass wall. All metal-glass connections were made by means of platinum joints. Two glass capillaries, one with a length of 9.60 cm and i.d. 322 μm, the other with a length of 9.80 cm and i.d. 156 μm, were investigated by recording $\Delta T = T_2 - T_1$ as a function of $\dot{Q}$.

3. Experimental results

Figure 2 gives the results of ΔT for the 322 μm capillary at two different bath temperatures, $T_b = 1.318$ K and $T_b = 1.257$ K. Figure 3 shows similar results for the 156 μm capillary at $T_b = 1.319$ K. The results have been plotted logarithmically as $-\rho s \Delta T$ against $v_n = \frac{4\dot{Q}}{\rho s T \pi d^2}$. For the temperature-dependent quantities ρ, s, and T their mean value at $T = \frac{1}{2}(T_1 + T_2)$ was used, thus taking into account their variation along the capillary up to third order in $\Delta T/T$.

The results show the general behaviour as also observed by Staas et al. and Van der Heijden et al. Two branches can be distinguished, one linear in v_n from which a transition to a second steeper branch occurs at an unpredictable value of v_n. This latter branch is then measured up to the highest velocity shown, upon which the heat input is decreased again and the curve traced down to $v_n = 0$ (see arrows in Figure 3). The reason that such high values of v_n could be measured as compared to those for other types of flow (see Chapter II) is that the response time of the system is now determined by its thermal properties only.

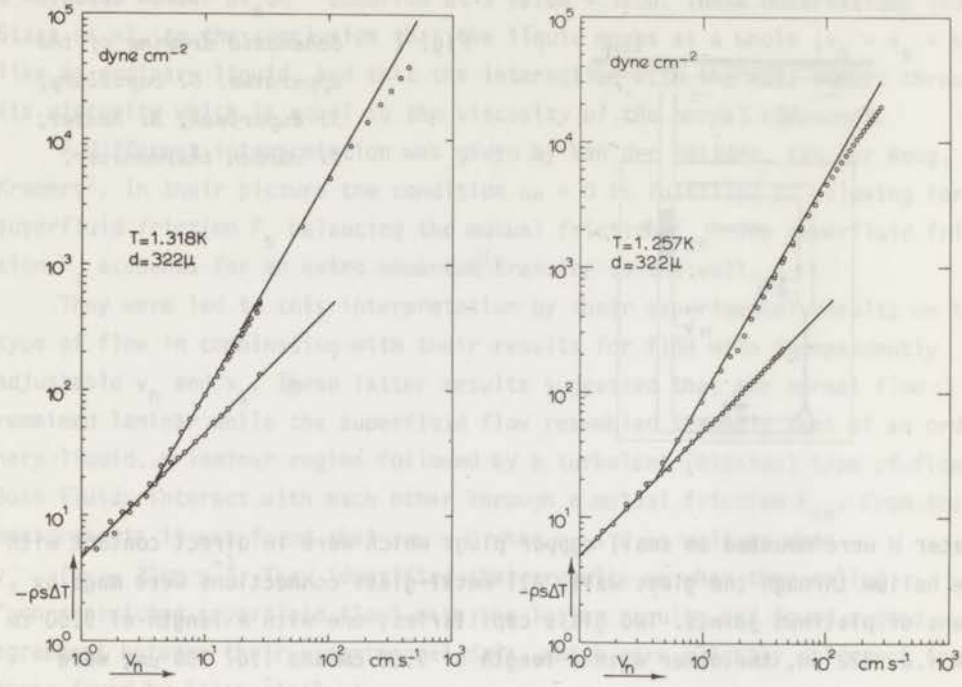

Fig. 2a,b *Double logarithmic plot of $-\rho_s \Delta T$ against v_n for the 322 μm i.d. capillary at the two bath temperatures. The drawn line with slope 1 is calculated according to the Poiseuille law, the other with slope 1.75 according to the Blasius law.*

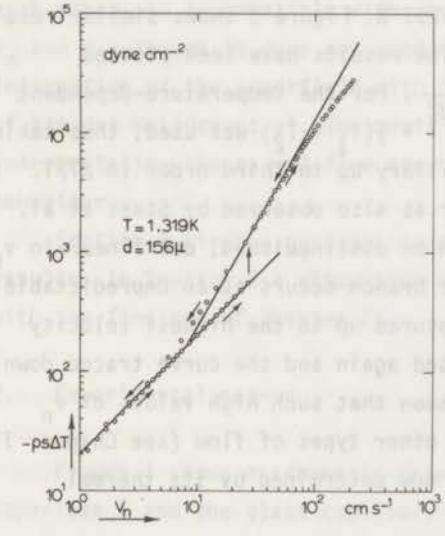

Fig. 3 *Double logarithmic plot of $-\rho_s \Delta T$ against v_n for the 156 μm i.d. capillary. The arrows in the figure indicate the sequence of the measurements.*

The drawn lines in the Figures correspond to the calculated Poiseuille law:

$$-\rho s \Delta T = \frac{32 \eta l}{d^2} v_n = -\Delta P_{Pois} \quad ,$$

and Blasius law:

$$-\rho s \Delta T = 0.158\, l \left[\frac{\rho^3 \eta v_n^7}{d^5}\right]^{1/4} = -\left[\frac{Re}{1189}\right]^{3/4} \Delta P_{Pois} \quad .$$

Their intersection corresponds to a Reynolds number $Re = \rho d v_n \eta^{-1} = 1189$. Generally speaking these lines give a fair description of the experimental results.

We extended the measurements to normal velocities higher than those investigated by Staas et al. and Van der Heijden et al. and found that in this region deviations occur; at the highest velocity (corresponding to a Reynolds number $Re \approx 1.3 \times 10^5$) these deviations amount to about a factor of two. The deviations in the region near the intersection of the drawn curves, which show up clearest in Figure 3 for the narrow capillary, were also found by Van der Heijden et al. and led these authors to their above-mentioned interpretation.

In conclusion, our results do not fully agree with either of the phenomenological relations proposed by Staas et al. or by Van der Heijden et al. However, the experimental differences are rather subtle and on the basis of these results alone a definite conclusion about the validity of the two descriptions cannot be drawn.

4. Discussion of the results

The proposal of Van der Heijden et al. to identify what they called "non-restricted superfluid flow" with the situations where $\Delta\mu = 0$ during the flow at independently adjustable v_s and v_n seems very sound. It is true that the correspondence is not one to one; for a given v_n there is more than one value of v_s leading to $\Delta\mu = 0$, but this explains the existence of two branches found for this type of flow.

It should be noted that in the steady-state solutions proposed so far a net circulation of superfluid is present in the circuit, even for the solutions on the linear branch. In view of the conservation-law of circulation one should raise the question of how this circulation could have slipped into the closed circuit.

From the successful analysis given by Van der Heijden et al. follows

already that this circulation does not impose severe restrictions on the flow. It is confirmed by a similar analysis that can be given on the basis of the data in Chapter II for the 216 μm capillary. Figures 4 and 5 give these data in three-dimensional graphs of $\rho\Delta\mu$ and $-\rho s\Delta T$ as a function of the transport velocities v_{cap} and v_n for the two bath temperatures T_b = 1.326 K and T_b = 1.054 K. From the Figures 4a and 5a the combinations (v_{cap}, v_n) are determined for which $\rho\Delta\mu = 0$. The corresponding value of $-\rho s\Delta T$ is then found from Figures 4b and 5b. The results are plotted in Figure 6. Experimental results on $\Delta\mu = 0$ flow not being available for this capillary, the curves representing the

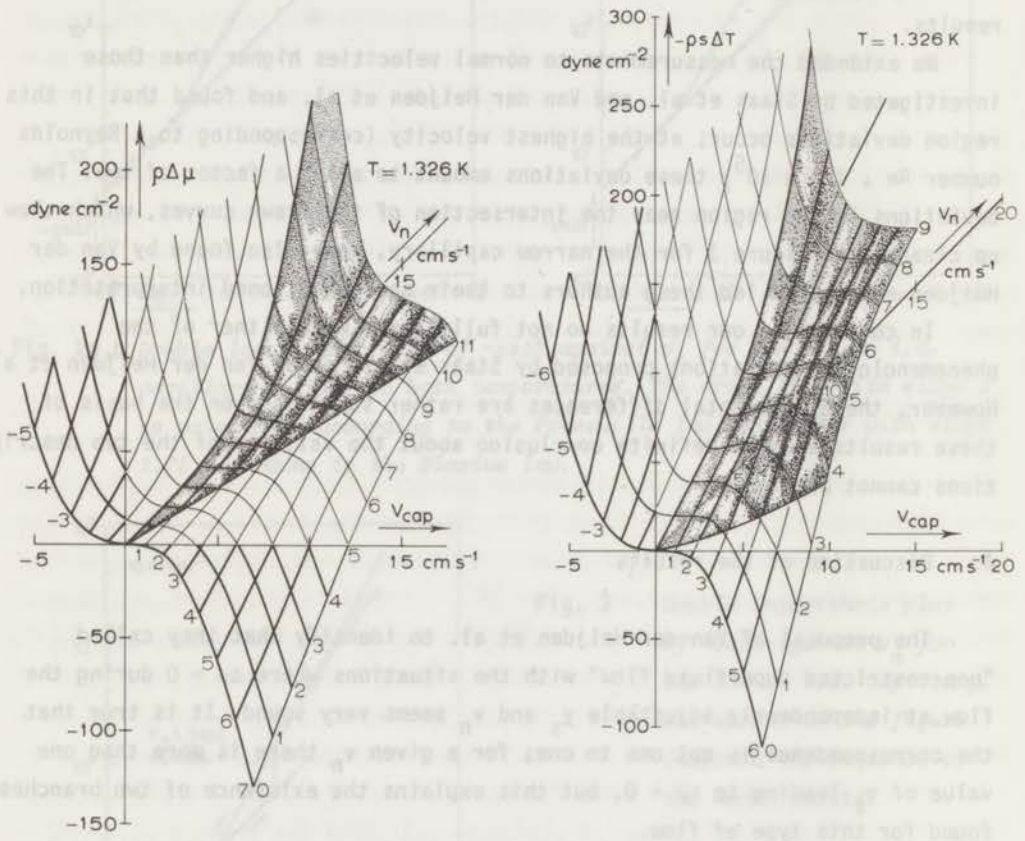

Fig. 4a,b *Three-dimensional graphs of $\rho\Delta\mu$ and $-\rho s\Delta T$ against (v_{cap}, v_n) at T = 1.326 K for flow with independently adjusted transport velocities (Chapter II). The shaded area indicates the positive part of the surface for which both v_{cap} and v_n are positive. The numbers in the graph indicate the values of v_{cap} respectively v_n.*

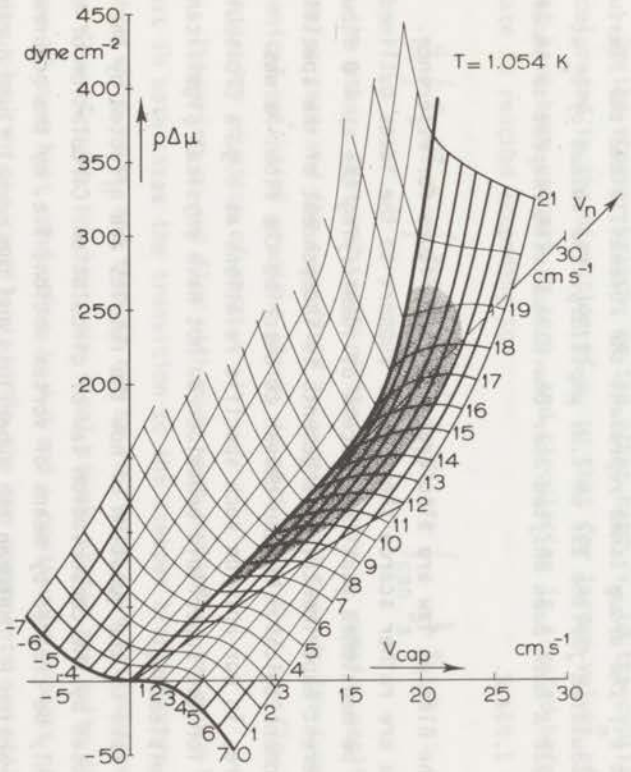

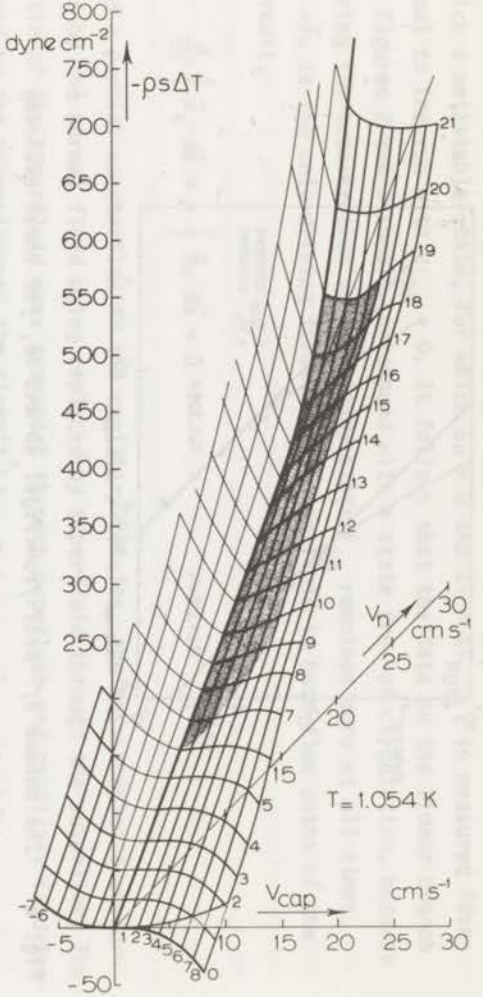

Fig. 5a,b

Three-dimensional graphs of ρΔμ and -ρsΔT against (v_{cap}, v_n) at T = 1.054 K for flow with independently adjusted transport velocities (Chapter II). Different from Figs. 4a and b the shaded area here indicates the region in which oscillations in the flow occur. The numbers in the graph indicate the value of v_{cap} respectively v_n.

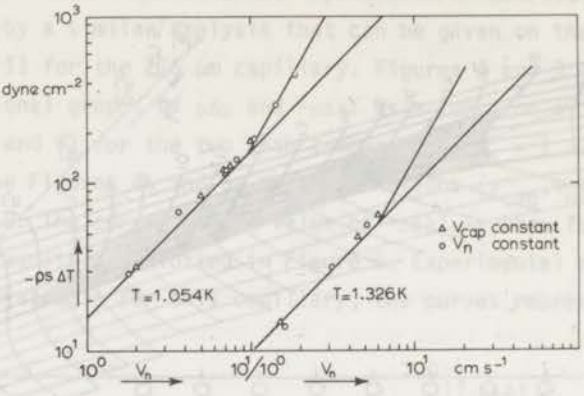

Fig. 6 *The values of $-\rho s \Delta T$ from Figs. 4b and 5b, for those velocity combinations (v_{cap},v_n) for which $\rho\Delta\mu = 0$ in Figs. 4a and 5a, plotted against v_n. The drawn lines represent the Poiseuille and the Blasius law calculated for the 216 μm i.d. capillary. The values of v_n at T = 1.326 K have been shifted over one decade with respect to those at T = 1.054 K.*

Poiseuille and the Blasius law are also drawn in this Figure for reference. Although the data are rather scarce they render support to the ideas outlined above. It should be mentioned that the success of identifying the $\Delta\mu = 0$ flow for the two different experimental arrangements is independent of the specific form of the phenomenological relations chosen to describe the flow. As was pointed out before, in our opinion such specific relations as e.g. a "Poiseuille and Blasius law" for the superfluid behaviour do not have physical significance and can be very misleading.

We will now take up the question of how the results are affected by the restrictions imposed by the conservation law of circulation. Circulation of the superfluid can only be created by means of vortex motion, i.e. by the occurrence of a mutual interaction F_{sn} between the superfluid and the normal fluid during the acceleration to the steady state. The three-dimensional plots of the steady-state values of $\rho\Delta\mu$ against v_{cap} and v_n shown in Figures 4a and 5a in fact represent $-\frac{\rho}{\rho_s} F_{sn}$ integrated over the capillary, since in the steady state $-\rho_s\Delta\mu = \int F_{sn} dl$.

From the plot for T_b = 1.326 K in Figure 4a we deduce that $\rho\Delta\mu = 0$ (at least experimentally indistinguishable from zero) not only for pure counterflow ($v_{cap} = 0$) but also in a region for sufficiently small v_{cap}. Indeed, Figure

10a of Chapter II shows a run at $T_b = 1.326$ K with $v_{cap} = \pm 1.10$ cm s^{-1} in which a metastable state, for which $\Delta\mu = 0$ and $\Delta T = \Delta T_{Pois}$, is measured identical to the run with $v_{cap} = 0$. It follows that the data on the linear branch in Figures 2 and 3 should correspond with a state free of circulation, because during the acceleration to the steady state F_{sn} remained zero at all times. As $-\vec{\nabla}\mu$ is the only driving force on the superfluid in both flow paths of the circuit,

$$\frac{d}{dt} \oint \vec{v}_s \cdot d\vec{s} = - \oint \vec{\nabla}\mu \cdot d\vec{s} = 0$$

and a partial counterflow in the capillary results, the mass-surplus transported by the normal fluid being replaced by superfluid through the superleak. The ratio of the superfluid mass transport through superleak and capillary is determined by the dimensions of the circuit*.

On the steeper branch, on the other hand, v_s in the capillary has been accelerated in the direction of v_n so that for larger values of (v_n, v_s) F_{sn} must have been unequal to zero, and circulation is created before the steady state is reached according to

$$\frac{d}{dt} \oint \vec{v}_s \cdot d\vec{s} = - \oint \vec{\nabla}\mu \cdot d\vec{s} - \oint \frac{1}{\rho_s} F_{sn} ds = - \int_{cap} \frac{1}{\rho_s} F_{sn} ds \quad .$$

In the other, "return", path of the flow where v_n remains negligible, F_{sn} remains zero and the superfluid is accelerated towards the superleak by the chemical-potential gradient alone, in such a way that the flow obeys the continuity equation of mass.

Comparing $\Delta\mu = 0$ flow with pure heat conduction we would like to remark that in both cases the transition to the steeper branch occurs at an unpredictable value of v_n and that it can be initiated by a disturbance from outside the flow circuit. However, the final steady states are quite different. In the case of pure heat conduction $\Delta\mu \neq 0$ and a continuous process of vortex motion takes place in the capillary, while the two components are still in counterflow.

---

* Note that the above description of the $\Delta\mu = 0$ flow also applies to the proposal of Ginzburg, Zharkov, and Sobyanin[3] to observe the thermomechanical circulating effect in superfluid helium. The description of the heat-conduction experiment of two parallel capillaries of different dimensions as given by these authors is incorrect, as no allowance is made for the occurrence of a partial counterflow in the capillaries.

For the $\Delta\mu = 0$ flow, on the other hand, no net vortex flow is present and the superfluid is moving in the direction of the normal transport.

In both cases the final states on the steeper branch show a definite persistence, a return to the linear branch can only be accomplished by reducing the heat input down to a low value. The mechanism responsible for this persistence is again quite different for the two cases. For pure heat conduction the vortex process, already present, provides sufficient disturbance of the flow to be maintained upon decreasing $\dot{Q}$. For $\Delta\mu = 0$ flow the persistence arises from the fact that in the final states the superfluid velocity is such that the mutual interaction $F_{sn} = 0$. When v_n is varied by a variation of $\dot{Q}$, F_{sn} temporarily becomes unequal to zero in such a way that the superfluid velocity is readjusted to the new value where again $F_{sn} = 0$. It follows from this picture that the return to the linear branch upon decreasing $\dot{Q}$ in the case of $\Delta\mu = 0$ flow takes place only when the subcritical region is reached, where F_{sn} is indistinguishable from zero. Note that upon a subsequent increase of $\dot{Q}$ the linear branch will be traced again, but now with a small amount of circulation frozen into the circuit*.

In the case of pure heat conduction, however, the return to the linear branch occurs when the vortex process is no longer able to maintain itself upon decreasing $\dot{Q}$. In the usual heat conduction experiment, where no mass transport is involved in reaching a new steady state, this is sometimes found to happen at values of v_n lying beyond the region where the linear and the steeper branch seem to touch[4]. In our experimental arrangement as described in Chapter II, however, the return to the linear branch can only be accomplished via flow states with $v_{cap} < 0$. As F_{sn}, i.e. the vortex process, increases for increasing negative values of v_{cap} and constant v_n, the tendency of the vortex process to disappear is counteracted. For this reason the steeper branch could be traced all the way down to the linear branch in our "open" apparatus.

Finally, we would like to remark that for $T_b = 1.054$ K a subcritical region (where F_{sn} remains zero in the presence of a small mass transport) is not observed when the flow is driven by the plungers. This is shown in Figure 5a and more clearly in Figure 11b of Chapter II, where F_{sn} is found to be unequal to zero even for the smallest value of $v_{cap} = 1.14$ cm s^{-1}. Moreover, the general shape of the curves for $-F_{sn}$ against v_{cap} is rather different from those at $T_b = 1.326$ K; a maximum in $-F_{sn}$ shows up which gives rise to the

---

* This description is consistent with the experimental finding that only very small bulk persistent currents can be created[5].

observed oscillations (see Chapter II). The question thus arises whether or not such a subcritical region does exist at these low bath temperatures, i.e. whether or not for sufficiently small v_{cap} also at this bath temperature a metastable state can be realized for which $F_{sn} = 0$. Such a state has been observed for pure heat conduction ($v_{cap} = 0$). It therefore seems plausible that it will also exist for small v_{cap}, especially for small positive v_{cap} when both v_s and $v_s - v_n$, responsible for the occurrence of a vortex process, are smaller in partial counterflow than for $v_{cap} = 0$. That it has not been observed should then be caused by the disturbance caused by the motion of the plungers. A good way to investigate this problem is to measure the $\Delta\mu = 0$ flow in a closed circuit also at these low bath temperatures. The appearance of a metastable linear branch, showing up clearest at high values of v_n, would give the answer to this problem. The measurements of Staas et al. confirm the presence of such a metastable state at the lower temperatures.

We finally conclude that $\Delta\mu = 0$ flow in a closed circuit is fully understood in terms of the steady flow behaviour at independently adjustable v_s and v_n.

References

1. Staas, F.A., Taconis, K.W. and Van Alphen, W.M., Physica 27 (1961) 893 (Commun., Leiden, No. 328d).
2. Van der Heijden, G., Van der Boog, A.G.M. and Kramers, H.C., Physica 77 (1974) 487 (Commun., Leiden, No. 411c).
3. Ginzburg, V.L., Zharkov, G.F. and Sobyanin, A.A., JETP Lett. 20 (1974) 97.
4. Childers, R.K. and Tough, J.T., J. low Temp. Phys. 15 (1974) 63.
5. Corke, H.E. and Hildebrandt, A.F., Phys. Rev. A2 (1970) 1492.

CHAPTER IV

SOME CONSIDERATIONS ON THE HYDRODYNAMICS OF THE FLOW

In the foregoing Chapters we have demonstrated that the different flow phenomena in capillary flow of He II can be deduced from the general results for steady flow presented in Chapter II. The question now remains what processes take place inside the capillary leading to the observed values of $\rho\Delta\mu$ and $\rho s\Delta T$.

It follows from the Landau equation of motion for the superfluid component[1]:

$$\frac{D_s}{Dt}\vec{v}_s = -\vec{\nabla}\mu \quad , \qquad \frac{D_s}{Dt} \equiv \frac{\partial}{\partial t} + \vec{v}_s\cdot\vec{\nabla} \quad , \tag{1}$$

that in our experiments the flow cannot really be stationary whenever $\Delta\mu \neq 0$ over the capillary. This statement does not change when the Landau equation is replaced by the more general dissipative equation of Khalatnikov[2]:

$$\frac{D_s}{Dt}\vec{v}_s = -\vec{\nabla}(\mu + H) \quad , \tag{2}$$

$$H = -\zeta_3\vec{\nabla}\cdot\rho_s(\vec{v}_s - \vec{v}_n) - \zeta_4\vec{\nabla}\cdot\vec{v}_n \quad , \tag{3}$$

ΔH over the capillary being zero as in the reservoirs the liquid is at rest.

As the superfluid transport is stationary this implies that the local superfluid velocity $\vec{v}_s$ as it appears in equation (1) can be considered as a steady transport velocity v_s, being the average of $\vec{v}_s$ in time and cross-section of the capillary, on which a non-steady superfluid circulation is superimposed[3]. The observed $\Delta\mu$ thus reflects a directed flow of circulation inside the capillary. As the circulation in He II can only be carried by quantized vortices[4] - the superfluid being irrotational except for a region near the vortex axis - the observed $\Delta\mu$ corresponds to a directed flow of vortices. According to the phase-slippage rule of Anderson[5]:

$$\Delta\mu = \kappa \dot{N} \quad , \tag{4}$$

where $\dot{N}$ is the net rate at which quantized vortices of circulation $\kappa = \frac{h}{m} \approx 10^{-3} cm^2 s^{-1}$ cross the entire flow path over which $\Delta\mu$ is measured. Anderson, who derived this rule from the rate of change of the phase of the internal order parameter†, showed that it can also be obtained directly from equation (1). For any fluid for which the equation of motion can be written as

$$\frac{D}{Dt}\vec{v} = -\vec{\nabla}\psi \quad , \qquad \frac{D}{Dt} \equiv \frac{\partial}{\partial t} + \vec{v}\cdot\vec{\nabla} \quad , \tag{5}$$

ψ being a scalar potential, it follows by integration between two points in the liquid that

$$\int_1^2 d\vec{l}\cdot\frac{\partial\vec{v}}{\partial t} - \int_1^2 (d\vec{l}\times\vec{v})\cdot(\vec{\nabla}\times\vec{v}) = -\Delta(\psi + \tfrac{1}{2}\vec{v}^2) \quad . \tag{6}$$

For quasi-steady flow, i.e. flow for which the transport velocity remains constant or varies slowly with time, equation (6) averaged over a suitable period T reads as:

$$-\langle\Delta(\psi + \tfrac{1}{2}\vec{v}^2)\rangle_T = \frac{1}{T}\left(\left(\int_1^2 d\vec{l}\cdot\vec{v}\right)_{t+T} - \left(\int_1^2 d\vec{l}\cdot\vec{v}\right)_t \right) - \left\langle\int_1^2 (d\vec{l}\times\vec{v})\cdot(\vec{\nabla}\times\vec{v})\right\rangle_T \tag{7}$$

If the variation in transport velocity is slow enough T can be chosen sufficiently long, so that equation (7) simplifies to

$$\langle\Delta(\psi + \tfrac{1}{2}\vec{v}^2)\rangle_T = \left\langle\int_1^2 (d\vec{l}\times\vec{v})\cdot(\vec{\nabla}\times\vec{v})\right\rangle_T \quad , \tag{8}$$

where the term $\Delta(\frac{1}{2}\vec{v}^2) = 0$ when the points 1 and 2 are chosen in quiescent

---

† Anderson showed that in the superfluid

$$\frac{\hbar}{m}\frac{\partial\phi}{\partial t} = \mu + \Omega + \tfrac{1}{2}\vec{v}_s^2$$

with ϕ the phase of the internal order parameter, μ the chemical potential, and Ω a possible external potential. Taking the gradient and integrating this relation between the reservoirs, and recognizing that every time a vortex passes the integration path the phase difference changes by 2π, one is immediately led to relation (4).

regions. In order to recognize the right hand side of equation (8) it should be remembered that for a fluid obeying equation (5), the well-known Kelvin theorem applies

$$\frac{D}{Dt} \oint d\vec{l} \cdot \vec{v} = 0 \quad , \tag{9}$$

the circulation around any closed contour moving with the fluid is conserved. From this theorem the Helmholtz theorem follows, i.e. the vorticity travels with the fluid. Therefore, the right hand side of equation (8) represents the net rate at which circulation crosses the chosen integration path between 1 and 2, or in a quasi-steady state any integration path between 1 and 2 for that matter. Applying this result to the case of He II, obeying equation (1) or rather equation (2) throughout the fluid, the result equation (4) is obtained as the circulation is transported solely by the quantized vortices.

This result, equation (4), provides a mere translation of the observed $\Delta\mu$'s in terms of vortex motion. It does not tell us anything about the mechanism responsible for the creation of vortices, nor does it predict how $\dot{N}$ is determined by the transport velocities of the superfluid and normal components. Moreover, as the Kelvin theorem requires that vortices move with the local superfluid velocity at the vortex axis, one could wonder how they ever can cross all "stream lines" in the flow path. This apparent paradox is easily resolved, however, by reading the Kelvin theorem in the other way, i.e. that the superfluid velocity at the core is imposed by the vortex motion. As has been shown by Putterman[6] the vortex motion itself is strongly influenced by the interaction with the normal component, that leads to a dissipative contribution to the vortex velocity. Therefore, Anderson's rule owes its physical significance to the presence of the normal component only.

It will thus be clear that vortex motion plays an important role in the interpretation of the experimental results. As has been shown by Putterman the motion of a vortex line element is governed by the value of the external velocities at the vortex axis. The external superfluid velocity results from a superposition of the velocity fields of the transport current and of all other vortices and images. The vortex velocity can be calculated from the decrease in free energy of the system as it follows from the Khalatnikov equations, no extra parameters are required (see Appendix).

Anderson's rule, which applies to all steady flow phenomena, imposes severe restrictions on possible hydrodynamic models. For instance the theory of Hall and Vinen[7], which meets with remarkable success[8] in the description of the

experimental results on pure heat conduction in He II, does not satisfy this rule. In this theory an equilibrium length of vortex lines per unit volume determined by the relative transport velocities of both components, serves as a handle for the superfluid to exchange momentum with the normal, thus giving rise to a mutual friction force in the equation of motion. Only when it can be proved that the rate of vortex transport is proportional to the equilibrium length of vortex lines, the agreement with the experimental results has physical significance.

The most successful theory in explaining the hydrodynamics of the flow in He II is the fluctuation theory of Langer and Fisher[9] (LF) as applied to flow in restricted geometries for which the normal transport velocity is zero. This theory satisfies Anderson's rule and there seems to be no reason why it should not also apply to capillary flow, certainly for flow with $v_n = 0$. Langer and Fisher consider superfluid flow in a closed circuit of length l and cross-sectional area A. The circulation in such a metastable flow-state is quantized in units κ. Due to thermal fluctuations there is a finite probability for the flow to lower its circulation by one unit. The rate R at which these processes take place is given by

$$R = Al\nu_o \exp[-E_a/k_BT] \quad , \tag{10}$$

where E_a is the activation energy for the process to occur which decreases with increasing velocity, and ν_o is a frequency per unit volume estimated to be of the order of the number of atomic collisions, $\nu_o \approx 10^{35}\,cm^{-3}s^{-1}$. As at every event the velocity of the superfluid decreases by κ/l the decay of the flow is given by

$$\frac{dv_s}{dt} = -\kappa A\nu_o \exp[-E_a/k_BT] \quad . \tag{11}$$

Independent of the specific value of E_a equation (11) shows the characteristic behaviour observed experimentally: up to a "critical velocity" the decay remains unmeasurably small, while above this velocity a logarithmic decay results[10,11].

The value of the activation energy E_a is determined by the kind of process by which the quantum of circulation slips out of the circuit. It is usually estimated from the dynamics of simple vortex processes, such as the expansion of vortex rings or vortex-line pairs by the flow. Above a critical radius respectively distance vortex rings or pairs of proper orientation will expand and cross the entire flow path. The activation energy is taken equal to the vortex energy at the critical size. Especially the vortex-line pair model is

in fair agreement with experiment[12], although the frequency ν_0 is found to be several orders smaller than the estimated value of $10^{35}cm^{-3}s^{-1}$. This does not seem unsatisfactory as it requires many atomic processes to increase one vortex ring or pair to its critical size.

The above theory is also applied successfully to film flow driven from one reservoir to another[13]. Superfluid flow in such an arrangement is also regarded as a metastable flow state from which again transitions to a lower state can occur at a rate given by equation (10). In order to maintain steady flow a driving force is required which according to Anderson's rule is given by

$$\Delta\mu = \kappa A l \nu_0 \exp[-E_a/k_B T] \quad . \tag{12}$$

Relation (12) shows the qualitative features of film flow observed experimentally, as for instance a critical velocity almost independent of the dimensions A and l in the film.

Although the LF-theory was originally developed for the temperature region close to T_λ, its applicability seems to extend to much lower temperatures[14]. It is found that the activation energy is of the form $E_a = \beta\rho_s v_s^{-1}$, as it is for the vortex ring model, but the constant β must be considered as an adjustable parameter, which turns out to be much smaller than its value for the vortex ring model. Moreover, ν_0 can be found[15] to be as small as $10^{17}cm^{-3}s^{-1}$.

There seems to be no reason to expect the LF-theory not to apply to capillary flow as well. However, the interesting question can be raised how an imposed normal transport velocity will affect the result (12). If the transition rate between metastable flow states is indeed determined by the activation energy as calculated from a classical vortex model, one expects a simple shift of the $\Delta\mu \leftrightarrow v_s$ curves, v_s being replaced by $v_s - v_n$ as follows by considering the local vortex processes in a reference frame moving with the normal fluid. However, regarding the process as a transition between two metastable flow states of the system as a whole, a transformation to a reference frame moving with the normal fluid affects the boundary conditions and one must expect that the absolute values of both velocities enter into the problem. It must be concluded that an extension of the LF-theory to cases with $v_n \neq 0$ cannot be obtained by simply using an activation energy as calculated from a classical vortex model.

We are therefore restricted to a comparison of our data on capillary flow with $v_n = 0$, with the LF-theory (Chapter I and Section 3.1 of Chapter II). None of the characteristic features such as an apparent critical velocity followed by a steep rise in $\Delta\mu$ are observed. The observed rise of $\Delta\mu \sim v_s^3$ is much too

slow. It must therefore be concluded that the LF-theory does not apply to capillary flow.

Nevertheless, thermal fluctuations should play a crucial role in the creation process of the vortices, as was pointed out by Campbell[16]. That the activation energy proves to be so small in capillary flow as compared to film flow or flow in narrow pores ($\lesssim$ 1000 Å), indicates that inhomogeneous nucleation of vorticity obtains. However, this inhomogeneous nucleation is not likely to be due to for instance the roughness of the wall of the capillary. Not only should one expect these effects to be much more pronounced for flow in narrow pores but also the agreement between the data obtained in different metal and glass capillaries seems to rule out this possibility. From the occurrence of a metastable branch with $\Delta\mu = 0$, as is found for pure heat conduction, it is rather suggested that the inhomogeneous nucleation takes place in the bulk of the liquid inside the capillary. Once vorticity is produced, for instance by a mechanical vibration of the flow circuit, it is maintained. The mere presence of vorticity is sufficient for new vortices to be created. This process may bear the explanation of the success of the Vinen theory.

Whatever the creation process of the vortices, the motion of the individual vortices is markedly different when they are driven by the normal transport as compared to when they are driven by the superfluid transport. The difference arises from the Poiseuille profile for the observed laminar normal flow for which $v_{n,//} \to 0$ close to the wall. A vortex driven by the normal fluid cannot reach this wall, and can therefore not contribute to the generated $\Delta\mu$ unless v_n is large enough for the image force to become effective. This would explain the occurrence of a critical value of v_n for pure heat conduction below which $\Delta\mu$ is identically zero. However, this does not explain the observation that, at the lower bath temperatures, a positive maximum in $\Delta\mu$ occurs when a small parallel superfluid transport is superimposed (Fig. 9b of Chapter II), because v_s would reduce the expansion of the vortex. The latter observation rather suggests that the number of vortices produced when $v_s = 0$, is zero. It seems therefore that superfluid motion is required for the creation process of the vortices, in agreement with our earlier conclusion that on the stable branch for pure heat conduction the superfluid motion induced by the vortices already present stimulates new vortices to be formed.

In conclusion, the vortex model able to explain the details of the observed $\Delta\mu(v_s, v_n)$ must be rather complicated. The present data in combination with Anderson's rule provide a severe test for the validity of any future model.

References

1. Landau, L.D., J. Phys. USSR 5 (1941) 71. (See also ref. 2, part V.)
   Landau, L.D. and Lifshitz, E.M., Fluid Mechanics, Pergamon Press (London, 1959) Ch. 16.
2. Khalatnikov, I.M., An Introduction to the Theory of Superfluidity, Benjamin (New York, 1965) Ch. 9.
3. Huggins, E.A., Phys. Rev. A1 (1970) 332.
4. Onsager, L., Suppl. Nuovo Cimento 6 (1949) 249.
   Feynman, R.P., Progr. low Temp. Phys., North-Holland Publ. Comp. (Amsterdam, 1955) Vol. I, Ch. II.
5. Anderson, P.W., Rev. Mod. Phys. 38 (1966) 298.
6. Putterman, S.J., Superfluid Hydrodynamics, North-Holland Publ. Comp. (Amsterdam, 1974) Ch. III, §32.
7. Hall, B.E. and Vinen, W.F., Proc. Roy. Soc. A238 (1956) 215.
   Vinen, W.F., Proc. Roy. Soc. A242 (1957) 493.
8. Tough, J.T. and Childers, R.K., Proc. XIV Int. Conf. low Temp. Phys., Otaniemi, Finland 1 (1975) 227.
9. Langer, J.S. and Fisher, E.F., Phys. Rev. Letters 19 (1967) 560.
10. Clow, J.R. and Reppy, J.D., Phys. Rev. Letters 19 (1967) 291.
    Verbeek, H.J., Van Spronsen, E., Van Beelen, H., De Bruyn Ouboter, R. and Taconis, K.W., Physica 77 (1974) 131.
11. Kukich, G., Henkel, R.P. and Reppy, J.D., Phys. Rev. Letters 21 (1968) 197.
12. Langer, J.S. and Reppy, J.D., Progr. low Temp. Phys., North-Holland Publ. Comp. (Amsterdam, 1970) Vol. VI, Ch. I.
13. See for instance: Proc. XIII Int. Conf. low Temp. Phys., Boulder, Colorado 1 (1972) part 4.
14. Notarys, H.A., Phys. Rev. Letters 22 (1969) 1240.
15. Liebenberg, D.H., Phys. Rev. Letters 26 (1971) 744.
16. Campbell, L.J., J. low Temp. Phys. 8 (1972) 105.

APPENDIX

From the decrease in free energy Putterman[1] derives the equation for the velocity $\vec{v}_l$ of a line element of vortex, orientated perpendicular to $\vec{v}_n$ and $\vec{v}_{se}$:

$$\vec{\kappa}\cdot[(\vec{v}_n - \vec{v}_{se}) \times (\vec{v}_l - \vec{v}_{se})] = 2\pi\zeta_3\rho_s(\vec{v}_{se} - \vec{v}_n)^2 \quad , \tag{1}$$

with ζ_3 one of the bulk viscosity coefficients introduced by Khalatnikov[2]. The component of $\vec{v}_l - \vec{v}_{se}$ perpendicular to $\vec{v}_{se} - \vec{v}_n$ is:

$$(\vec{v}_l - \vec{v}_{se})_\perp = 2\pi\zeta_3\rho_s\kappa^{-2}\vec{\kappa} \times (\vec{v}_n - \vec{v}_{se}) \quad . \tag{2}$$

Vortex motion is often described in the literature by the vector equation introduced by Hall and Vinen[3]:

$$\rho_s\vec{\kappa} \times (\vec{v}_l - \vec{v}_{se}) = \nu(\vec{v}_l - \vec{v}_n) + \frac{\nu'}{\kappa}\vec{\kappa} \times (\vec{v}_l - \vec{v}_n) \tag{3}$$

with the coefficients ν and ν' determined by the scattering process of the excitations with the core of the vortex, their values still being in discussion[4]. Equation (3) can be rewritten in the form:

$$\rho_s\vec{\kappa} \times (\vec{v}_l - \vec{v}_{se}) =$$

$$= \frac{\rho_s^2\kappa^2\nu}{\nu^2+(\rho_s\kappa-\nu')^2}(\vec{v}_{se} - \vec{v}_n) - \rho_s\frac{\nu^2-\nu'(\rho_s\kappa-\nu')}{\nu^2+(\rho_s\kappa-\nu')^2}\vec{\kappa} \times (\vec{v}_{se} - \vec{v}_n) \quad . \tag{4}$$

Equation (4) is thus compatible with equation (2) if one identifies:

$$\zeta_3 = \frac{\kappa^2}{2\pi}\frac{\nu}{\nu^2 + (\rho_s\kappa-\nu')^2} \quad . \tag{5}$$

For further identification one needs to know the component of $\vec{v}_l - \vec{v}_s$ parallel to $\vec{v}_{se} - \vec{v}_n$. If, when $\vec{v}_n = 0$, one takes:

$$(\vec{v}_l - \vec{v}_{se})_{//} = 0 \quad , \tag{6}$$

i.e. the vortex velocity is a superposition of the external superfluid velocity $\vec{v}_{se}$ and a dissipative contribution (equation (2)) perpendicular to $\vec{v}_{se}$, the vortex velocity for the general case $\vec{v}_n \neq 0$ becomes:

$$\vec{v}_l - \vec{v}_{se} = 2\pi\zeta_3\rho_s\kappa^{-2}\vec{\kappa} \times (\vec{v}_n - \vec{v}_{se}) \quad . \tag{7}$$

Identification of equation (4) with equation (7) leads to expressions for ν and ν' in terms of ζ_3 as:

$$\nu = \frac{\kappa^2}{2\pi\zeta_3}[1 + (\frac{\kappa}{2\pi\rho_s\zeta_3})^2]^{-1} \qquad \nu' = \rho_s\kappa[1 + (\frac{\kappa}{2\pi\rho_s\zeta_3})^2]^{-1} \quad . \tag{8}$$

Using these results it seems justified to use the convenient expression (3) as the equation of motion for vortices of arbitrary orientation with respect to $\vec{v}_{se}$ and $\vec{v}_n$.

References

1. Putterman, S.J., Superfluid Hydrodynamics, North-Holland Publ. Comp. (Amsterdam, 1974) Ch. III, §32.
2. Khalatnikov, I.M., An Introduction to the Theory of Superfluidity, Benjamin (New York, 1965) Ch. 9.
3. Hall, B.E. and Vinen, W.F., Proc. Roy. Soc. A238 (1956) 215.
4. Sonin, E.B., Proc. XIV Int. Conf. low Temp. Phys., Otaniemi, Finland 1 (1975) 181.

SAMENVATTING

Na de ontdekking van de superfluiditeit van vloeibaar helium aan het einde van de dertiger jaren, zijn vele experimenten uitgevoerd met het doel de stromingseigenschappen van het He II te onderzoeken. Men tracht, met als uitgangspunt het voor reversibele verschijnselen in He II zo succesvol gebleken tweefluida model, de irreversibele eigenschappen te beschrijven door in de bewegingsvergelijkingen voor het massa transport van beide componenten wrijvingstermen op te nemen. Uit de experimenteel bepaalde waarden van deze wrijvingstermen als functie van de transportsnelheden wordt dan getracht het hydrodynamische gebeuren in de stroming af te leiden. Het is niet verwonderlijk dat deze procedure geleid heeft tot uiteenlopende beschrijvingen voor de locale gebeurtenissen, temeer daar - met uitzondering van het onderzoek van Van der Heijden et al. - nooit in één experiment alle relevante uitwendige parameters gevarieerd zijn. Zo is bijvoorbeeld gepoogd een algemeen model te ontwikkelen uitsluitend op grond van resultaten van warmtegeleidingsmetingen, waarbij een koppeling tussen de beide transportsnelheden optreedt omdat het totale massa transport nul is.

De in dit proefschrift beschreven onderzoekingen zijn er op gericht in één experiment de eigenschappen bij stationnaire capillaire stroming systematisch als functie van de onafhankelijk gevarieerde transportsnelheden van de superfluide en normale component te bepalen en te laten zien dat de resultaten van meer specifieke stromingsexperimenten hierin begrepen zijn. In hoofdstuk II wordt dit systematische onderzoek - uitgevoerd bij twee badtemperaturen T = 1.326 K en T = 1.054 K - beschreven. Twee reservoirs zijn verbonden door een circuit bestaande uit een superlek en een glazen capillair, die in een vacuumkamer zijn gemonteerd. Met behulp van verdringers in de reservoirs wordt een massa transport door het capillair in stand gehouden. Op dit massa transport wordt een warmtestroom gesuperponeerd door met een kacheltje tussen superlek en capillair te stoken; op deze wijze kan in het capillair een transport van de normale component naar believen worden ingesteld. In stationnaire toestand wordt het resulterende verschil in chemische potentiaal en temperatuur over het capillair gemeten. De experimentele resultaten blijken in goede overeenstemming te zijn met de resultaten van Van der Heijden.

De metingen aan het superfluide transport in metalen capillairen ingesloten tussen twee superlekken, zoals beschreven in hoofdstuk I, zijn uitgevoerd om de afhankelijkheid van de resultaten van de geometrie van het capillair en de aard van het materiaal van de wand te onderzoeken. Uit deze meer specifieke experimenten is gebleken dat de gemeten verschillen in chemische potentiaal en temperatuur recht evenredig zijn met de lengte van het capillair. Uit een vergelijking met de resultaten voor superfluide transport in het glazen capillair (hoofdstuk II, sectie 1) kan worden geconcludeerd dat de stromingseigenschappen ongevoelig zijn voor de diameter en de aard van de wand van het capillair.

In hoofdstuk III wordt een tweede specifiek stromingsexperiment besproken. In een gesloten circuit waarin het superlek en het capillair zijn opgenomen, wordt met behulp van het kacheltje een normaal transport ingesteld. Alleen het temperatuurverschil over het capillair wordt gemeten, daar het chemisch-potentiaal verschil in stationnaire toestand identiek nul is. De resultaten van ΔT blijken inderdaad in goede overeenstemming te zijn met de verwachting gebaseerd op de resultaten van stroming met $\Delta\mu = 0$ gegeven in hoofdstuk II.

Bij de algemene metingen van hoofdstuk II zijn in het snelheidsgebied voor kleine parallele superfluide en normale transporten regelmatige oscillaties in de gemeten $\Delta\mu$ en ΔT gevonden. Er wordt aangetoond dat ook het optreden van dit bijzondere stromingsverschijnsel kan worden begrepen op grond van het algemene stromingsgedrag.

Hoewel een synthese tussen de verschillende stromingsverschijnselen in termen van de transportsnelheden dus mogelijk is gebleken, is hiermee het locale hydrodynamische gebeuren in de stroming nog geenszins duidelijk. De macroscopisch experimenteel bepaalde grootheden zijn uiteraard slechts een grove maat voor de locale variaties, maar zij kunnen zeker dienen als criterium voor de geldigheid van locale hydrodynamische modellen. In hoofdstuk IV wordt er op gewezen dat bewegende superfluide wervels in het capillair een essentiele rol spelen; het stationnaire chemisch-potentiaal verschil is recht evenredig met het aantal superfluide wervels, dat het gehele stroompad doorsnijdt, onafhankelijk van de vraag hoe dit aantal door de transportsnelheden wordt bepaald. De meetresultaten wijzen er op dat (ten gevolge van thermische fluctuaties) circulatie gecreëerd wordt door inhomogene nucleatie in de vloeistof, hetgeen gestimuleerd wordt door de locale superfluide snelheid.

Teneinde te voldoen aan het verzoek van de Faculteit der Wiskunde en Natuurwetenschappen volgt een beknopt overzicht van mijn studie.

Na in 1961 het eindexamen gymnasium B aan het R.K. Lyceum St. Bonaventura te Leiden te hebben afgelegd, begon ik mijn studie aan de Faculteit der Wiskunde en Natuurwetenschappen aan de Rijksuniversiteit te Leiden. Ik legde in 1966 het candidaatsexamen af met hoofdvakken natuurkunde en wiskunde en bijvak sterrenkunde en in 1969 het doctoraalexamen met hoofdvak natuurkunde en bijvak mechanica.

Inmiddels was ik sinds 1966 werkzaam op het Kamerlingh Onnes Laboratorium, als assistent op het natuurkunde practicum voor pre-candidaten en als medewerker in de groep die thans onder leiding staat van Prof. Dr. K.W. Taconis, Prof. Dr. R. de Bruyn Ouboter en Dr. H. van Beelen. Aanvankelijk assisteerde ik Dr. W.M. van Alphen bij metingen over de dissipatie van superfluide helium en over persisterende massastromen. Mijn eerste zelfstandige onderzoek dateert uit 1968 met een experiment waarin de invloed van de capillairlengte op de energiedissipatie bij superfluide transport werd onderzocht. Spoedig werd dit experiment uitgebreid door tegelijkertijd het temperatuur- en chemisch potentiaal verschil over het capillair te meten. De metingen aan het experiment met superfluide én normaal transport werden in de nachten van 1974 uitgevoerd, waarbij ik overdag geassisteerd werd door Drs. A. Hartoog.

Ik spreek mijn erkentelijkheid uit voor de prettige medewerking die ik van de staf van het laboratorium heb ondervonden. Met name, de metaal-technische assistentie van de heren J.P. Hemerik, A.J.J. Kuyt en G. Vis en de glas-technische assistentie van de heer P.J.M. Vreeburg.

De uiteindelijke vorm van dit proefschrift is in niet geringe mate bepaald door Dr. H. van Beelen; zijn stimulerende kritische philosophie bij het interpreteren van meetgegevens heeft een blijvende indruk op mij gemaakt.

6. [illegible] bestudeerden de magnetische fase-overgangen in $MnCl_2 \cdot 4H_2O$ met behulp van differentiële susceptibiliteits-metingen. Zij gaan er echter ten onrechte van uit dat deze meetresultaten altijd de isotherme [illegible]

7. Het is mogelijk met behulp van ^3He-gas metingen [illegible]

8. In de litteratuur wordt [illegible] een te optimistische voorstelling gegeven van [illegible]

9. Mackinnon beweert dat de ongewone eigenschappen van vloeibaar helium-gas [illegible]

L. Mackinnon, Experimental Physics at low Temperatures, [illegible]

10. Het in augustus 1978 door de Regering bij de Tweede Kamer in behandeling [illegible]

11. Op de spreekkaartjes die uitgaan van de Consultatiebureaus voor Zuigelingen [illegible]

12. Het gebruik van [illegible] tegenwoordig de [illegible] moet worden.

25 november 1978 [illegible]

STELLINGEN

1. Over het thermomechanische circulatie-effect in superfluide helium, analoog aan het thermoelectrische effect in supergeleidende metalen ringen, wordt ten onrechte beweerd dat de superfluide circulatie ongelijk nul is.

   V.L. Ginzburg, G.F. Zharkov en A.A. Sobyanin, JETP Letters 20 (1974) 97.

   Pagina 63 van dit proefschrift.

2. Het is onbegrijpelijk dat de formules van Fresnel voor de amplitude van gereflecteerd licht, gepolariseerd parallel aan en loodrecht op het invalsvlak, sinds 1827 in de literatuur over de optica consequent met verschillend teken worden gegeven.

   M. Born en E. Wolf, Principles of Optics, Pergamon Press (London, 1965) p. 40.

3. De beschrijving van superfluiditeit en supergeleiding uitsluitend als gevolg van de ononderscheidbaarheid van bosonen, waardoor er een sterke neiging zou bestaan voor de deeltjes dezelfde toestand te bezetten, verdient kritische aandacht.

   R.P. Feynman, R.B. Leighton en M. Sands, The Feynman Lectures on Physics, Addison-Wesley Publ. Co. (Reading, 1963) Vol. III p. 4-12, 21-8.

4. Het is gewenst de balansvergelijking voor het impulsmoment bij de afleiding van de bewegingsvergelijking in de hydrodynamica niet onbesproken te laten.

   S.J. Putterman, Superfluid Hydrodynamics, North-Holland Publ. Co. (Amsterdam, 1974).

5. De afleiding van de relatie tussen de inductie-spanning en het aangelegde magnetische veld voor een harde supergeleider van de tweede soort, zoals gegeven door Eckert en Berthel, is niet correct.

   D. Eckert en K.H. Berthel, Cryogenics 15 (1975) 479.

6. Rives en Benedict bestuderen de magnetische fase-overgangen in $MnCl_2 \cdot 4H_2O$ met behulp van differentiële susceptibiliteits-metingen. Zij gaan er echter ten onrechte van uit dat deze meetresultaten altijd de isotherme susceptibiliteit opleveren.
   J.E. Rives en V. Benedict, Phys. Rev. B12 (1975) 1908.

7. Het is mogelijk met behulp van ^{3}He-gas metingen met de gasthermometer uit te voeren in het temperatuurgebied tussen 1 K en 2 K.

8. In de literatuur wordt soms een te optimistische voorstelling gegeven van de mogelijkheid een commerciele SQUID met een "fluxtransformator" te gebruiken voor directe metingen van de susceptibiliteit of de magnetische temperatuur.
   O.V. Lounasma, Experimental principles and methods below 1 K, Academic Press (London, 1974) p. 225.

9. Mackinnon beweert dat de ongewone eigenschappen van vloeibaar helium pas 24 jaar na de eerste vloeibaar-making duidelijk werden. Zijn verklaring hiervoor, namelijk dat er op het Kamerlingh Onnes Laboratorium een voorkeur bestond voor metalen boven glazen dewars, is nonsens.
   L. Mackinnon, Experimental Physics at low Temperatures, Wayne State University Press (Detroit, 1966) p. 41.

10. Het in augustus 1975 door de Regering bij de Tweede Kamer in behandeling brengen van het ontwerp van wet strekkende tot opheffing van de evenredige vrachtverdeling kreeg een provocerend karakter, daar het wegens het geringe aanbod van lading de schippers toen onverschillig kon zijn of zij werkeloos in een binnenhaven dan wel in de Nieuwe Waterweg lagen.

11. Op de oproepkaarten die uitgaan van de Consultatiebureaus tot Bestrijding der Tuberculose dient men tevens te wijzen op het gevaar dat bestraling kan opleveren bij zwangerschappen van minder dan twee weken.

12. Het gebruik van levend aas is onverenigbaar met de geest waarin tegenwoordig de vissport beoefend moet worden.

19 november 1975

W. de Haas